Trinity College Dublin
Coláiste na Tríonóide, Baile Átha Cliath
The University of Dublin

# Functional characterisation of the small RNA Arp in *Acinetobacter baumannii* and the development of a programmable sRNA to modulate carbapenem resistance

MSc Molecular Microbiology thesis 2026

by

**Orla Connell**

**Moyne Institute of Preventive Medicine Department of Microbiology Trinity College Dublin,**
**The University of Dublin**

## Declaration

I declare that this thesis has not been submitted as an exercise for a degree at this or any other university and it is entirely my own work. I confirm that the work has been completed in full compliance with relevant university policies, including the Academic Integrity policy, the Trinity Policy on Good Research Practice, and the guidance on AI and GenAI in Teaching, Learning, Assessment and Research.

I agree to deposit this thesis in the University's open access institutional repository or allow the Library to do so on my behalf, subject to Irish Copyright Legislation and Trinity College Library conditions of use and acknowledgement.

I consent to the examiner retaining a copy of the thesis beyond the examining period, should they so wish (EU GDPR May 2018).

**Orla Connell 29/09/2025**

**Acknowledgments**

I would like to thank my supervisor Asst. Prof. Carsten Kröger for hosting me in his lab and the incredible guidance and advice he provided throughout my masters project. I would also like to thank the members of the Kröger lab, Fergal, Rebecca and Orlaith for helping me every step of the way and being so friendly throughout my time in the lab. I would also like to express my gratitude to all the staff and members of the Moyne Institute for being so welcoming and helpful. I would like to thank my family for supporting me through this journey. Lastly, I have to acknowledge my friends Tapasya, Elizabeth, Ciara and Weronika who made my time as a postgraduate unforgettable, it would not have been the same without their support and friendship.

**Publications:**

Aalap Mogre, **Orla Connell**, Jessica White, Ali Shaibah, Karsten Hokamp, Fergal J. Hamrock, Kristina Schauer, Carsten Kröger

Development of two compatible plasmids to assess sRNA-mediated post-transcriptional regulation in *Acinetobacter baumannii*

PMID: 41288586

PMCID: PMC12646401

DOI: 10.1099/mic.0.001639

Fergal J. Hamrock, Thomas Guest, Mikaela N. Daum, **Orla Connell**, Anna S. Ershova, Karsten Hokamp, Alastair B. Fleming, Michael J. Gebhardt, Alexander J. Westermann, Carsten Kröger

DNA uptake and twitching motility are controlled by the small RNA Arp through repression of pilin translation in Acinetobacter baumannii

bioRxiv 2025.07.19.665661; doi: https://doi.org/10.1101/2025.07.19.665661

**Summary**

The World Health Organisation's number one critical priority pathogen *Acinetobacter baumannii (A. baumannii)* is a Gram-negative bacterium which can cause multi-drug resistant infections, particularly pneumonia, bloodstream and wound infections. This bacterium has developed resistance to last-line antibiotics such as carbapenems, which calls for the discovery of new treatments and understanding these mechanisms of resistance. *A. baumannii* succeeds as a pathogen due to its persist and resist mechanisms, partially due to the plasticity of the bacterium's genome. Bacterial regulatory small RNAs (sRNAs) are crucial for responding to the changing environment through the quick fine tuning of gene expression at a post transcriptional level. They can activate or repress the translation of certain genes via antisense base pairing in response to stressors in the environment, allowing for the bacteria's survival. Until recently, the post-transcriptional landscape of multi-drug resistant *A. baumannii* had remained unclear.

In this study, the sRNA Arp which was recently uncovered through Hi-GRIL-seq, was validated to bind the target mRNA *pilA* which is a major component in type IV pili in *A. baumannii* AB5075. Arp was then functionally characterised as a repressor of the type IV pili phenotypes twitching motility and DNA uptake. The second part of this study investigated the potential of an RNA based therapy to treat carbapenem resistant *A. baumannii*. Small regulatory RNAs have been used as a blueprint for the creation of RNA based antibiotics such as antisense oligonucleotides (ASOs). These antibiotics target essential genes in pathogenic bacteria, repressing the translation of genes involved in crucial pathways and killing the bacteria. This study used the new plasmid toolkit pAMCK to validate other known sRNA-mRNA interaction pairs in *A. baumannii* AB5075. One of the tested sRNAs Aar was chosen as a sRNA scaffold for the development of the programmable sRNA Aar-oxa23, which aimed to re-sensitise *A. baumannii* to already available carbapenem antibiotics. The sRNA has an altered seed region which targets and represses the translation of the carbapenem resistance gene Oxa-23 in *A. baumannii*. This proved to reduce the protein levels of Oxa-23 and therefore reduce *A. baumannii's* resistance to the carbapenems imipenem and meropenem. These results highlight important insights into *A. baumannii* sRNA mediated regulation mechanisms, as well as advances in sRNA therapeutics, such that the alteration of the

short seed region is sufficient to target and produce the desired effect on the target mRNA.

# Table of Contents

# Introduction

## *Acinetobacter baumannii* is a multidrug resistant nosocomial pathogen

The genus *Acinetobacter* comprises at least 33 species, most of which are naturally found in soil and water, while only a minority act as opportunistic pathogens (Towner, 2009). *Acinetobacter baumannii (A. baumannii)* is a Gram negative bacterium that is the most significant nosocomial *Acinetobacter* pathogen (Peleg *et al.*, 2008). Unlike other species, *A. baumannii* is mostly isolated from hospitals but its' natural reservoir is unclear (Ahuatzin-Flores *et al.*, 2024). This bacterium belongs to the ESKAPE group of pathogens (*Enterococcus faecium, Staphylococcus aureus, Klebsiella pneumoniae, Acinetobacter baumannii, Pseudomonas aeruginosa and Enterobacter spp)*, known for being multi-drug resistant (De Oliveira *et al.*, 2020). *A. baumannii* is a pathogen of global concern, spreading rapidly throughout hospitals in the USA and Europe, with even higher rates of infection reported in Asia and the Middle East (Mathai *et al.*, 2012, Chung *et al.*, 2011, Agodi *et al.*, 2010, Rodríguez-Baño *et al.*, 2004).

*A. baumannii* typically causes infections in critically ill and immunocompromised patients, particularly in intensive care units (ICUs) (García-Garmendia *et al.*, 2001, Blanco *et al.*, 2017). Patients in ICUs are highly susceptible to *A. baumannii* infections due to weakened immune systems, recent surgeries, trauma and the use of invasive medical devices (Jiang *et al.*, 2022). These infections are commonly linked to mechanical ventilation, causing ventilator associated pneumonia (VAP) or bloodstream infections (BSI) and urinary tract infections caused by intravenous and urinary catheters (Jaruratanasirikul *et al.*, 2019, Bandić-Pavlović *et al.*, 2020, Jang *et al.*, 2009, Pour *et al.*, 2011, Hazen *et al.*, 2023). A recent meta-analysis revealed that hospital-acquired *A. baumannii* infections had a concerningly high mortality rate, at ~43% (Mohd Sazlly *et al.*, 2019). *A. baumannii* can also cause skin and soft tissue infections from colonising sites of trauma or burn wounds (Tekin *et al.*, 2014, Johnson *et al.*, 2007). This was particularly a problem for soldiers during war in Iraq and Afghanistan who experienced multi-drug resistant *A. baumannii* wound infections from military combat (Scott *et al.*, 2007, Keen *et al.*, 2010, Davis *et al.*, 2005).

The rise of antibiotic resistance is making these infections extremely difficult to treat. Of particular concern, is carbapenem resistant *A. baumannii* (CRAb), as carbapenems are often last resort antibiotics for multi-drug resistant infections (Poirel & Nordmann, 2006). As a result, CRAb has been ranked the number 1 critical priority pathogen on the World Health Organisation (WHO) priority list of antibiotic resistant bacteria to guide research and development of new antibiotics (Sati *et al.*, 2025).

**Carbapenem resistant *Acinetobacter baumannii* (CRAb)**

Carbapenems are a class of beta-lactam antibiotics which inhibit bacterial penicillin binding proteins (PBPs) with a broad spectrum of activity in both Gram-negative and Gram-positive bacteria. They are often used as a last-line treatment for multi-drug resistant infections, however resistance to carbapenems has been on the rise (Da Silva & Domingues, 2016). Bacterial carbapenem resistance can arise from a combination of outer membrane modifications, antibiotic efflux via efflux pumps and reduced membrane permeability (de Souza *et al.*, 2025). However, an analysis of global *A. baumannii* isolates revealed that the main driver of carbapenem resistance was the widespread acquisition of $bla_{\text{Oxa-23-like}}$ carbapenemase genes (Mack *et al.*, 2025). Carbapenemases are a type of beta-lactamase, enzymes which hydrolyse the beta-lactam moiety of these antibiotics and render them inactive (Smith *et al.*, 2013). Four classes of beta-lactamases exist, class A include extended-spectrum beta-lactamases (ESBLs), class B are metallo-beta-lactamases (MBLs), class C are AmpC beta-lactamses and class D are OXA-type beta-lactamases (carbapenemases) including OXA-23 (Ambler, 1997). Between 2000 and 2024, the prevalence of these carbapenemases increased by approximately 45% worldwide (Mack *et al.*, 2025). Carbapenem resistance is spreading rapidly in *A. baumannii* with recent data from the WHO Global Antimicrobial Resistance and Use Surveillance System (GLASS) dashboard in 2022 showing that of all *Acinetobacter* bloodstream infections, 89% showed carbapenem resistance (de Souza *et al.*, 2025).

The first carbapenem resistant *A. baumannii* strain was found in Scotland in 1985 and the protein responsible was deemed "ARI-1" for "*Acinetobacter* resistant to imipenem" and later identified as Oxa-23 (Donald *et al.*, 2000, Paton *et al.*, 1993). *A. baumannii* has an intrinsic Oxa-type enzyme, Oxa-51, which is encoded on the chromosome, however Oxa-23 is an acquired gene and often plasmid encoded (Evans & Amyes, 2014, de Souza *et*

*al.*, 2025). Oxa-23 is a membrane bound protein in *A. baumannii* and can be found in outer membrane vesicles (Capodimonte *et al.*, 2024). Oxa-23 and other Oxa enzymes are often incorporated with insertion sequences (IS) such as ISAba1 or ISAba3 which enhance gene expression by providing strong promoter sequences, increasing carbapenem resistance (de Souza *et al.*, 2025). These IS elements can also facilitate horizontal gene transfer encouraging the spread of Oxa genes (Evans & Amyes, 2014). Due to selective pressure and horizontal gene transfer of resistance determinants, treatment options are hindered and mortality and morbidity rates are increased (Da Silva & Domingues, 2016). Since the emergence of CRAb, there is a lack of treatment options for these types of infections and there is a need for new therapeutics, such as beta lactamase inhibitors (Bush & Bradford, 2020).

**Persistence and resistance*: A. baumannii* has a plastic genome**

The ability of *A. baumannii* to survive and thrive in nosocomial environments is due to its persistence and resistance mechanisms (Roca *et al.*, 2012). *A. baumannii* can persist in harsh environments for long periods of time, resisting desiccation and disinfectants. This is due to a number of factors such as the ability to form biofilms on biotic and abiotic surfaces such as plastic and glass, which are often parts of medical devices (Espinal *et al.*, 2012). The success of *A. baumannii* as a nosocomial pathogen is also largely due to its plastic genome, which can quickly and easily adapt and respond to stressful environments (Harding *et al.*, 2018). This genetic plasticity has allowed for the quick development of antimicrobial resistance, through mutation and the incorporation of mobile genetic elements (Kyriakidis *et al.*, 2021). The evolution of *A. baumannii* genome has involved the incorporation of virulence and antibiotic resistance genes via horizontal gene transfer from the environment (Touchon *et al.*, 2014). The ability to explore the environment and uptake and incorporate environmental DNA involves type IV pili (T4P) (Harding *et al.*, 2013).

***A. baumannii* Type IV pili (T4P) are essential for horizontal gene transfer and motility**

Due to a lack of flagella, *A. baumannii* has been known to be non-motile, with its name deriving from “akineto”, meaning non-motile in Greek (McBride Mark, 2010). However,

*A. baumannii* has been found to have Type IV pili (T4P) which are involved in a type of movement called twitching motility (Henrichsen & Blom, 1975, Eijkelkamp *et al.*, 2011). Twitching motility was first described as a flagella independent surface movement in *A. calcoaceticus* (Mattick, 2002). Twitching motility is mediated by the extension and retraction of T4P which involves many pilin genes, including *pilA*, the major subunit for the formation of T4P (Harding *et al.*, 2013, Mattick *et al.*, 1996). This study also showed that *A. baumannii* T4P are involved in DNA uptake (Harding *et al.*, 2013). *A. baumannii* is naturally competent, allowing for the uptake of environmental DNA, genomic recombination and horizontal gene transfer of virulence factors such as antibiotic resistance determinants (Godeux *et al.*, 2022). These phenotypes are interconnected, with DNA uptake being shown to be linked to movement along wet surfaces (Wilharm *et al.*, 2013).

**Post transcriptional regulation in Gram-negative bacteria**

In order for bacteria to survive, they must quickly adapt to changing environments and external threats such as antibiotics and toxins. To quickly respond, gene expression must be regulated by the bacteria for an appropriate response to thrive in the environment. RNA-mediated regulation of gene expression is vital to this, it can involve both coding RNAs which are translated into proteins and non-coding RNAs which are not translated but still play a functional role (Chauvier & Walter, 2024). Small regulatory RNA (sRNA) are a type of short non-coding RNA (50-250 nucleotides) which act as post-transcriptional regulators and are crucial for bacteria (Storz *et al.*, 2011). sRNAs can help bacteria cope with environmental stress, by fine tuning the expression of genes involved in different pathways such as metabolism and antibiotic resistance (Gottesman *et al.*, 2006, Dersch *et al.*, 2017). sRNAs usually consist of three functional domains, a base pairing sequence for binding of RNA, an RNA-binding protein (RBP) site for chaperones such as Hfq and lastly a Rho independent terminator site (Papenfort & Melamed, 2023).

sRNAs can act as *trans* or *cis*-regulatory elements. *Cis* encoded sRNA are more commonly found in Gram-positive bacteria (Waters & Storz, 2009). *Cis* sRNAs are transcribed from the complementary strand of the mRNA they regulate and the regulatory mechanism involves base pairing with fully complementary regions in the RNA transcript of the gene they regulate. Both the sRNA and target transcripts are transcribed as discreet

RNA species and function as diffusible molecules which have complementarity of 75 nucleotides or more (Waters & Storz, 2009). *Trans* encoded sRNA are transcribed in a location separate to the mRNA they regulate and work through imperfect antisense base pairing but involve specific seed sequences (Papenfort *et al.*, 2010). *Trans* acting sRNA primarily bind to the 5' untranslated region (UTR) or further into the coding region of target mRNAs, occluding the ribosome binding site (RBS) inhibiting translation of the target mRNA **(Figure 1)** (Waters & Storz, 2009). The sRNA-mRNA duplex may then be degraded by RNase E, making the regulation irreversible (Waters & Storz, 2009). *Trans* sRNAs can also activate target mRNA translation through anti-antisense base pairing which relieves an inhibitory secondary structures, revealing the RBS or sequestering RNase E binding site (Urban & Vogel, 2008). Many *trans*-acting sRNA also have the ability to bind and regulate multiple transcripts (Hör *et al.*, 2018). Gram-negative *trans* encoded sRNA often involve RNA binding proteins (RBP) such as the RNA chaperone Hfq (Waters & Storz, 2009). The RNA chaperone brings the sRNA and mRNA close together allowing the pairing to occur and protecting the RNA from degradation (Valentin-Hansen *et al.*, 2004). In 1984, the first bacterial regulatory sRNA that functions through base-pairing was discovered, MicF in *E. coli* which inhibits translation of OmpF, an outer membrane porin (Mizuno *et al.*, 1984). Since then RNA biology techniques have advanced and more regulatory sRNAs have been identified.

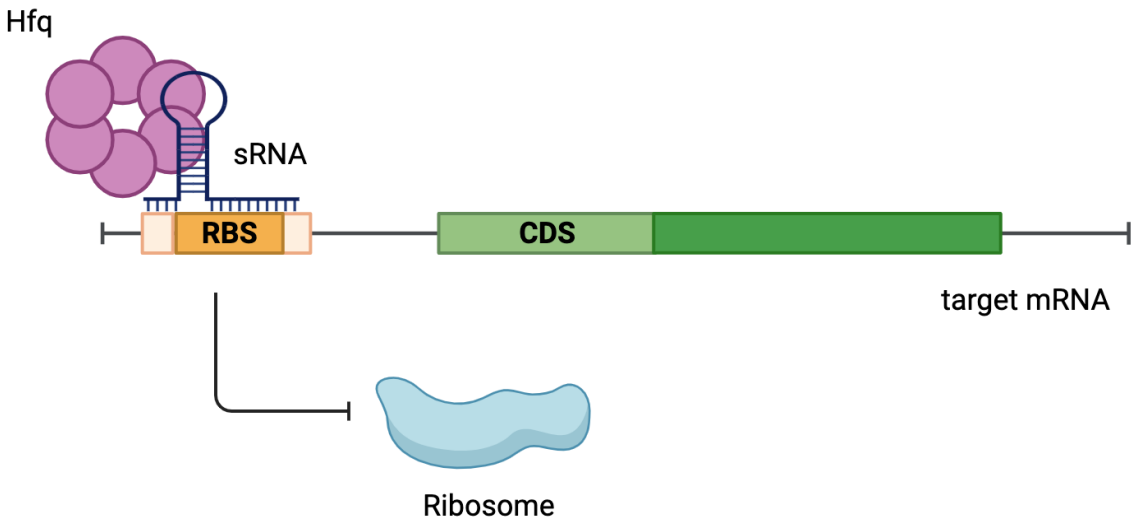


**Figure 1: Mechanism of post-transcriptional gene regulation via Hfq-associated *trans*-encoded sRNAs.** Regulatory sRNA inhibit target mRNA translation via base pairing with the ribosome binding site (RBS), preventing the 30S ribosome subunit from binding and translating the transcript.

### *A. baumannii* AB5075 is a contemporary model strain

Research has primarily been conducted using the American Type Culture Collection strains of *A. baumannii,* ATCC 19606 or ATCC 17978, isolated in 1948 and 1951, however there was a need for a more recent and significantly antibiotic resistant strain. *A. baumannii* AB5075 is a contemporary multi-drug resistant strain that was isolated from a wound infection in 2008 (Jacobs *et al.*, 2014). It serves as a model strain for *A. baumannii* pathogenesis due to its virulence in animal models and its genetic tractability (Jacobs *et al.*, 2014). *A. baumannii* AB5075 remains susceptible to certain antibiotics such as apramycin and tetracycline, making it compatible with genetic manipulation (de Dios *et al.*, 2022).

### Small regulatory RNAs in *A. baumannii*

The study of bacterial sRNAs has mostly been developed in *Escherichia coli* (*E. coli*) and *Salmonella enterica,* which serve as model organisms in the field of sRNA biology. In these organisms, numerous sRNAs have been characterised, including the *Salmonella* sRNA RybB which regulates outer membrane proteins (OMP) translation and the *E. coli* sRNA RyhB which regulates the translation of iron utilisation genes (Papenfort *et al.*, 2010, Papenfort *et al.*, 2006, Massé & Gottesman, 2002, Johansen *et al.*, 2006). In contrast, the RNA regulatory landscape of *A. baumannii* has until recently remained poorly understood compared with other Gram-negative bacteria (Sarshar *et al.*, 2022).

Initial insights into sRNA-mediated post transcriptional regulation came from the discovery of Aar (Amino acid regulator), the first sRNA identified in the non-pathogenic *A. baylyi*, which is conserved in *A. baumannii* (Schilling *et al.*, 2010). In 2014, novel regulatory sRNAs were uncovered in *A. baumannii* ATCC 17978 by screening of intergenic regions and confirmation via northern blot (Sharma *et al.*, 2014). The sRNAs were found to be induced under temperature and osmotic stress conditions and the sRNA AbR25 was suggested to play a role in efflux pump regulation and drug resistance (Sharma *et al.*, 2014). Subsequent transcriptomic studies in *A. baumannii* ATCC 17978 identified 110 sRNAs highlighting a diverse regulatory network (Kröger *et al.*, 2018). More recently, the sRNA AbsR28 was discovered in the same strain, which is involved in the regulation of the Type VI secretion system (T6SS) in a manganese-dependent manner (Bhowmik *et al.*, 2025). AbsR28 was found to base pair with *tssM* mRNA which encodes part of the T6SS, repressing this machinery when there is an excess of intracellular

manganese during oxidative stress (Bhowmik *et al.*, 2025). These discoveries gave insight into sRNA mediated regulation in the ATCC 17978 strain, however AB5075 was yet to be investigated. The first research into the sRNA landscape of the clinically relevant *A. baumannii* AB5075 involved the application of High-throughput Global sRNA Interaction by Ligation and Sequencing (Hi-GRIL-seq), which uncovered numerous novel sRNAs and mapped their mRNA targets, providing insight into post-transcriptional regulation in this pathogen (Hamrock *et al.*, 2024).

**Hi-GRIL-seq**

A challenge in RNA biology is determining the target mRNA of regulatory sRNA. Pairs can be identified bioinformatically or through experimental approaches such as high-throughput proximity ligation based methods such as RIL-seq or Hi-GRIL-seq (Hör *et al.*, 2018). Predication tools such as IntaRNA can identify sequence complementarity between known sRNAs and mRNA targets, taking into consideration secondary structures and base-pairing potentials and providing hybridization energy (Busch *et al.*, 2008). Previously sRNA target identification methods were performed using microarrays and then RNA sequencing, comparing differentially expressed genes of sRNA-deletion strains to wild-type bacterial strains (Papenfort *et al.*, 2008). Pulse over expression of the sRNA in the deletion strains was also used and the transcriptome was assessed (Papenfort *et al.*, 2006). These methods had many limitations including off-target effects, which can be partially resolved by incorporating sRNA seed region mutant controls in experiments (Gebhardt *et al.*, 2023). RIL-seq stands for RNA interaction by ligation and sequencing involving crosslinking of RNA-RBP complexes and co-immunoprecipitation (Melamed *et al.*, 2016). Hi-GRIL-seq is high-throughput global sRNA target identification by ligation and sequencing, it identifies sRNA-mRNA interactions independently of RBP and uses deeper sequencing resolution. This method uses the ectopic expression of T4 RNA ligase to create RNA-RNA chimeras of RNA molecules in proximity to each other, first used in *P. aeruginosa* and recently adapted for *A. baumannii* AB5075 (Hamrock *et al.*, 2024). Hi-GRIL-seq in *A. baumannii* AB5075 revealed 632 chromosomal sRNA chimeras and 74 plasmid derived RNA chimeras, including the interaction between the sRNA Aar and mRNA *carO* .

### *A. baumannii* compatible two plasmid system pAMCK

To investigate sRNA-mRNA interactions *in vivo*, a fluorescence reporter plasmid system may be used such as $pP_L$, pXG10, which validated sRNA interactions in *Salmonella enterica* and *E. coli,* however this system does not work in *A. baumannii* (Corcoran *et al.*, 2012, Urban & Vogel, 2007). A new genetic tool which aids the investigation of sRNA-mRNA interactions in *A. baumannii* is the pAMCK plasmid system (Mogre *et al.*, 2025). The newly designed plasmids fulfil the historical role of the $pP_L$ pXG10 translational reporter plasmid system. The newly made compatible plasmids have origins of replication pWH1266 and pRSF1010 which can be stably maintained in *A. baumannii* allowing for the validation of RNA-RNA interactions in this pathogen (Mogre *et al.*, 2025). Similar to the original system, these plasmids contain the identical constitutive $P_{LtetO}$ and $P_{LlacO}$ promoters and a truncated sfGFP to create translational fusions (Corcoran *et al.*, 2012, Mogre *et al.*, 2025, Urban & Vogel, 2007). The new plasmid system can be used to validate sRNA-mRNA interactions in *E. coli* and *A. baumannii,* as well as an overexpression vector to characterise the sRNA phenotypes.

### Programmable sRNA therapeutics

Due to the rise of antibiotic resistance, there is an urgent need for new narrow spectrum antibiotics. One therapeutic consideration is species-specific programmable RNA antibiotics (Vogel, 2020). These antisense oligonucleotides (ASOs) antimicrobials are short single strand oligomers mimicking DNA or RNA and bind complementary RNA, inhibiting translation or promoting degradation of target mRNA (Dias & Stein, 2002, Sully & Geller, 2016). These antibiotics work by inhibiting essential processes within the bacteria, causing death or arresting its life cycle. These gene-specific ASOs could target a single pathogen, keeping commensal bacteria intact (Vogel, 2020). Existing types of antisense antimicrobials include phosphorothioates (S-DNA), locked nucleic acids (LNA), peptide nucleic acids (PNA), and phosphorodiamidate morpholino oligomers (PMO) (Sully & Geller, 2016). PNAs are the most studies type of antisense therapy (Pifer & Greenberg, 2020). Since 1981, synthetic DNA analogues have been shown to inhibit growth of bacteria (Jayaraman *et al.*, 1981). However, the first FDA-approved antisense oligonucleotide therapy that targets a microorganism was Fomivirsen, a drug that treats

cytomegalovirus induced retinitis by intravitreal injection to AIDS patients (Sully & Geller, 2016, Orr, 2001).

Programmable synthetic sRNA are an attractive treatment option due to their precision targeting and specificity. The optimal length for ASOs is the same as natural sRNAs (50-200 nts). Natural *trans*-sRNA have seed regions of 8-12 bases which determine the search and pairing to the specific target mRNA (Gorski *et al.*, 2017). Specific genes in target pathogenic organisms can be chosen to be repressed resulting in reduction of fitness or death of the bacteria, without affecting commensal bacteria. Thanks to whole genome sequencing, identification of target genes and the design of ASOs is relatively simple. However it does not come without limitations (Vogel, 2020). ASOs cannot self-mediate entry into bacterial cells, therefore are often required to be attached to a cell-penetrating peptide (CPP), with cationic and non-polar amino acids (Xue *et al.*, 2018). Off target effects and toxicity to human cells must also be investigated, further complicating the process.

**Aims of this study**

The first aim of this thesis was to functionally characterise the *A. baumannii* AB5075 sRNA Arp by determining whether its interaction with *pilA* produces measurable phenotypic effects. To address this, the interaction was first be validated with the newly developed plasmid reporter system (pAMCK), followed by phenotypic experiments assessing twitching motility and DNA uptake.

The second aim was to create a synthetic programmable sRNA which represses carbapenemase mRNA Oxa-23 in *A. baumannii* AB5075. The pAMCK plasmid system was used as a toolkit to create this programmable sRNA. The effectiveness of this sRNA as an adjunctive therapy was tested via antibiotic susceptibility assays.

# Materials and methods

## Bacterial strains and growth conditions

Bacterial strains used in this study were *E. coli* TOP10 (Invitrogen), *A. baumannii* AB5075 (obtained from Salcedo Lab (Lyon, France)), *A. baumannii* Δ*arp*, *A. baumannii* Δ*aar*. For long term storage of strains, overnight cultures were combined with 30% (v/v) sterile glycerol and kept at -80 °C. Strains were streaked on lysogeny broth (L-agar (Lennox broth 1.5% w/v Bacto agar)) with necessary antibiotics and grown for 16-18 h in an incubator (Memmert) at 37 °C. Plates were stored at 4 °C for short term storage. Plates were used within 2 weeks of being streaked. For preparation of an overnight culture, a single colony was inoculated into 4 ml L-broth (lysogeny broth (Lennox): Bacto-tryptone (10 g/l), NaCl (5 g/l), Bacto-yeast extract (5 g/l) with antibiotic required to maintain plasmids. Overnight cultures were grown at 37 °C 200 rpm agitation in a shaking incubator (Labwit) for 16-18 h. To monitor the growth of bacteria, the optical density at wavelength 600nm ($OD_{600}$ )was measured using a GENESYS 10 spectrophotometer (Thermo Spectronic).

## Antibiotics

Antibiotics stocks were prepared at 1000x desired concentration, in 70% ethanol or water and filter sterilised with 0.2 µm PES membrane filter (Fisher Scientific). The antibiotics used in this study were tetracycline (12 µg/ml) and apramycin (60 µg/ml). Antibiotic containing plates were made by diluting antibiotics 1:1000 in molten L-agar ~55°C, then poured and cooled.

## Plasmids

Plasmids used and created in this study are listed in **Table 1**. Plasmids were stored in bacterial cryo-stocks with associated antibiotic at -80 °C.

**Table 1: Plasmids used in this study.**

| Plasmid | Description | Resistance | Source |
|---|---|---|---|
| pAMCK14-Arp | Arp overexpression vector for use in *E. coli* and *A. baumannii* translational reporter system | $Apra^R$ | This Study |
| pAMCK14-Arp* | Arp* overexpression vector for use in *E. coli* and *A. baumannii* translational reporter system | $Apra^R$ | This Study |
| pAMCK18-PilA | PilA-sfGFP expression vector for use in *E. coli* and *A. baumannii* translational reporter system | $Tet^R$ | This Study |
| pAMCK18-PilA* | PilA*-sfGFP expression vector for use in *E. coli* and *A. baumannii* translational reporter system | $Tet^R$ | This Study |
| pAMCK14-RyhB-2 | RyhB-2 overexpression vector for use in *E. coli* and *A. baumannii* translational reporter system | $Apra^R$ | This Study |
| pAMCK18-SodB | SodB-sfGFP expression vector for use in *E. coli* and *A. baumannii* translational reporter system | $Tet^R$ | This Study |
| pAMCK14-Aar | Aar overexpression vector for use in *E. coli* and *A. baumannii* translational reporter system | $Apra^R$ | This Study |
| pAMCK18-CarO | CarO-sfGFP expression vector for use in *E. coli* and *A. baumannii* translational reporter system | $Tet^R$ | This Study |
| pAMCK15 | Control vector for use in *E. coli* and *A. baumannii* translational reporter system | $Apra^R$ | This Study |
| pAMCK14-Aar-oxa23 | Aar-oxa23 overexpression vector for use in *E. coli* and *A. baumannii* translational reporter system | $Apra^R$ | This Study |
| pAMCK18-oxa23 | Oxa23-sfGFP expression vector for use in *E. coli* and *A. baumannii* translational reporter system | $Tet^R$ | This Study |

**Genomic DNA isolation**

Genomic DNA was isolated from *A. baumannii* and *Salmonella enterica* serovar Typhimurium 4/74 for use as a template in PCR. From an overnight culture, 400 µl was centrifuged at 21,100 x g for 1 min. The pellet was resuspended in 200 µl sterile water and boiled at 100 °C for 10 mins. This sample was vortexed and centrifuged at 21,100 x g for 5 mins. The supernatant was placed in a new tube and 200 µl of chloroform was added and centrifuged again at 21,100 x g for 10 mins at 4 °C. The aqueous phase was removed

and the DNA concentration was measured using the NanoDrop ND-1000 spectrophotometer (Thermo Scientific). The DNA was stored at -20 °C.

**Plasmid isolation**

Plasmids were isolated from overnight cultures of *E. coli* using the *EasyPure*® Plasmid MiniPrep Kit (Transgen Biotech). Cultures were pelleted by centrifugation at 13,000 x g for 1 min and plasmids isolated using manufacturers instructions. Plasmid concentration was determined via NanoDrop ND-1000 spectrophotometer (Thermo Scientific). Plasmids were stored at -20 °C.

**Preparation of calcium competent cells of *E. coli* TOP10**

A single colony of *E. coli* TOP10 was used to inoculate an overnight culture. The next day 50 µl of this overnight culture was used to inoculate 50 ml of L-broth in an Erlenmeyer flask (1:1,000 dilution). This culture was grown at 37 °C shaking until exponential phase was reached ($OD_{600}$ = 0.4 – 0.8). This was centrifuged at 2,000 x g at 4 °C for 8 min. The supernatant was discarded and the pellet was resuspended in 40 ml ice-cold $CaCl_2$ (0.1M). This was kept on ice for 20 min then centrifuged at 2,000 x g at 4 °C for 8 min. The supernatant was discarded and the pelleted was resuspended with 10 ml ice-cold $CaCl_2$ and 1.15 ml of 87% v/v glycerol. This was split into 300 µl aliquots in 1.5 ml tubes and stored at -80 °C.

**Polymerase chain reaction (PCR)**

Polymerase chain reactions were used to amplify plasmid inserts from genomic DNA and to amplify the plasmid backbones from plasmid stocks. PCR was carried out with forward and reverse primers, template DNA (gDNA 100ng/µl or plasmid DNA 20-50 ng/ µl), Verifi™ polymerase mix (PCR Biosystems) and deionised water. Volumes of PCR components are listed in **Table 2**. Cycling conditions used for PCR are in **Table 3.** Primers used in this study are listed in **Table 4.** PCR controls contained the same components except template DNA.

**Table 2: PCR component volumes**

| Component | Volume (µl) |
|---|---|
| Forward primer (10 µM) | 1 |
| Reverse primer (10 µM) | 1 |
| DNA template | 1 |
| Water | 22 |
| 2x Polymerase mix (VeriFi™) | 25 |
| Total | 50 |

**Table 3: PCR cycling conditions**

| Step | Temperature | Time | Cycles |
|---|---|---|---|
| Denaturation | 95 °C | 2 min | 1 |
| Denaturation | 95 °C | 15 s | 35 |
| Annealing | Variable | 30 s | |
| Extension | 72 °C | Variable | |
| Extension | 72 °C | 2 min | 1 |

**Table 4: PCR primer list**

| Primer name | Sequence 5'-> 3' | Description |
|---|---|---|
| BB_pPL_for | GTGCTCAGTATCTTGTTATCCGCTC AC | To amplify pAMCK14 backbone |
| BB_pPL_rev | TCTAGAGGCATCAAATAAAACGAA AGGC | To amplify pAMCK14 backbone |
| SLIC_pXG10sf_f | GCTAGCGGATCCGCTGGCTCCGCTG C | To amplify pAMCK18 backbone |
| BB_pXG10_rev | ATGCATGTGCTCAGTATCTCTATCAC | To amplify pAMCK18 backbone |
| pPL-sRNA40_dRNAseq_F | GTGAGCGGATAACAAGATACTGAG CACATCAAAAAGGATATATAATTCC | To amplify *arp* |
| pPL-sRNA40_R | GCCTTTCGTTTTATTTGATGCCTCTA GA TTTGAGTAGATATGAGAAGTC | To amplify *arp* |
| pXG10_pilA_F | ACTGAGCACATGCATAGCTGAAAA AGCTTATATAAAAAC | To amplify *pilA* |

| | | |
|---|---|---|
| pXG10_pilA_R | AGCGGATCCGCTAGCGGCAACTAC GATCATGAGTTCG | To amplify *pilA* |
| sRNA21_pPL_F | GTGAGCGGATAACAAGATACTGAG CACGTAGGTTGATATGAACC | To amplify *aar* |
| sRNA21_pPL_R | GCCTTTCGTTTTATTTGATGCCTCTA GAAGTTATCAAACAAAGGCGC | To amplify *aar* |
| pXG10_CarO_F | ACTGAGCACATGCATATGCTCTTGA ATATAATTTTTGTC | To amplify *carO* |
| pXG10_CarO_R | AGCGGATCCGCTAGCAAGTAAAGC TGTAGTTGTCAC | To amplify *carO* |
| RyhB-2_F | GATAACAAGATACTGAGCACAGCA CATCGTCAGGAAAGTG | To amplify *ryhB-2* |
| RyhB-2_R | TTTTATTTGATGCCTCTAGAGAAAA AAGACCATGAATTCG | To amplify *ryhB-2* |
| SodB_F | GAGATACTGAGCACATGCATACGCG CACCAGGGGTATTG | To amplify *sodB* |
| SodB_R | GAGCCAGCGGATCCGCTAGCCAGA GCATCTTTGGCATACG | To amplify *sodB* |
| Oxa-23 up – F (P1) | CCGGCTGCAACAATAGCTGC | To amplify fragment upstream of oxa-23 for deletion |
| Oxa-23 up -R (P2) | GGCCCAATTCGCCCTATAGTGAGTC GCTTATCTTAAACAAATCTCTAAAA TGG | To amplify fragment upstream of oxa-23 for deletion |
| Oxa-23 P3 | GGGTTTGCTCGGGTCGGTGGCATAT GGCTGAATATTATTTAAGAGCTTGA CAG | To amplify fragment downstream of oxa-23 for deletion |
| Oxa-23 P4 | GCGTTAGTTCACGAAGCTTGGCTTT TTGACC | To amplify fragment downstream of oxa-23 for deletion |
| P5 | CGACTCACTATAGGGCGAATTGGGC C GCTTTCCAGTCGGGAAACCTG | To amplify SacBaacC4 from gDNA |
| P6 | CATATGCCACCGACCCGAGCAAAC CCCGCCAGGGTTTTCCCAGTCACG AC | To amplify SacBaacC4 from gDNA |
| Oxa-23 insert v1 F | ACTGAGCACATGCATATAACTCATT GAG | To amplify oxa-23 variant 1 and 2 |

| | | |
|---|---|---|
| Oxa-23 insert v1 R | AGCGGATCCGCTAGCAACCACATAGC | To amplify oxa-23 variant 1 |
| Oxa-23 insert v2 R | AGCGGATCCGCTAGCAATAATATTCAGCTG | To amplify oxa-23 variant 2 |
| Aar oxa-23 F | CAAGATACTGAGCACGTAGGTTGATATGAACCTCACGACAAAACACCAGATCCCGAAACTGTTTTTAACAGA | To amplify Aar with sequence changed to bind oxa-23 |
| Pleu_qPCR_F | TTTCCCCGAAAAGTGCCACCTG | Sanger sequencing of pAMCK14 backbone |
| pCS26_PssrB_check_F | CCATTATTATCATGACATTAACC | Sanger sequencing of pAMCK18 backbone |

**PCR product purification**

PCR products which had correctly amplified the desired sequence were purified using the *EasyPure*® PCR product purification Kit (Transgen Biotech). The samples were processed via manufacturer's instructions. PCR product concentration was determined via NanoDrop ND-1000 spectrophotometer (Thermo Scientific). PCR products were stored at -20 °C.

**Colony PCR**

Colony PCR was used to confirm the presence of a specific DNA sequence in a bacterial colony. Taq polymerase and taq master mix was used to perform colony PCR. A toothpick was dipped into a colony and then into the PCR mix as template. The component volumes for colony PCR are listed in **Table 5**. The colony PCR cycling conditions are listed in **Table 6.**

**Table 5: Colony PCR components**

| **Component** | **Volume (µl)** |
|---|---|
| Forward primer (10 µM) | 0.5 |
| Reverse primer (10 µM) | 0.5 |
| Polymerase (Taq) | 0.5 |
| Taq Master Mix | 5 |
| DNA template | x |
| Water | 3.5 |
| **Total** | 10 |

**Table 6: Colony PCR cycling conditions**

| **Step** | **Temp** | **Time** | **Cycles** |
|---|---|---|---|
| Denaturation | 95 °C | 10 min | 1 |
| Denaturation | 95 °C | 15 s | 35 |
| Annealing | Variable | 30 s | |
| Extension | 72 °C | Variable | |
| Extension | 72 °C | 2 min | 1 |

**Agarose gel electrophoresis**

Agarose gels 1-2% (w/v) were used to confirm PCR products were the predicted size. Gels were made with agarose powder in 1x TAE buffer (40 mM Tris-acetate and 1 mM EDTA) and dissolved in the microwave. The molten gel was poured with combs to solidify. One µl of DNA loading dye was mixed with 3 µl of PCR product and pipetted into a well. Gels were run at 100 V for 25-30 min in 1x TAE buffer. DNA ladders were used to compare the size of DNA fragments. CSL-MDNA-1KBPLUS (Cleaver Scientific) ladder was used for DNA fragments > 1,000 bp and Hyperladder IV (Bioline) were used for DNA fragments < 1,000 bp. SYBR™ Safe DNA Gel Stain (Thermo Fischer scientific) was used to visualise bands on agarose gels and imaged under the safeVIEW-MINI2 blue light transilluminator (Cleaver Scientific).

### *Dpn*I digestion

Amplified linear plasmid backbone PCR products were *Dpn*I-digested with Anza™ 10 *Dpn*I (Invitrogen) to remove residual template plasmid DNA prior to performing SLiCE reactions. 1 µg of the PCR backbone product was incubated with 1 µl Anza™ 10x Buffer, 1 µl Dpn1 and sterile water up to 10 µl at 37 °C for 1 h.

### Plasmid construction

Seamless Ligation Cloning Extract (SLiCE) cloning was used to construct all plasmids for this study (Zhang *et al.*, 2012). This involved combining DNA inserts and plasmid backbones with SLiCE extract and incubating at 37 °C for 1 h. The components of the SLiCE reactions are listed in **Table 7.** The DNA inserts were amplified from genomic DNA using primers which add overhang regions to the insert. These overhangs consist of ~ 20 bp of homology to the linearised *Dpn*I digested plasmid backbone. This allows for recombination of the insert into the backbone and circularisation of the plasmid. The SLiCE product was transformed into calcium competent *E. coli* TOP10 cells. For cloning an insert into the pAMCK14 backbone, ~300 ng of linearised PCR amplified plasmid was used. For cloning of pAMCK18 backbone, ~500 ng of linearised PCR amplified backbone was used. As a SLiCE control, the same reaction was set up without insert DNA and transformed into *E. coli* to ensure template plasmids was digested by *Dpn*I.

**Table 7: SLiCE reaction components**

| **Component** | **pAMCK14 reaction** | **pAMCK18 reaction** |
|---|---|---|
| SLiC extract | 1 µl | 1 µl |
| T4 DNA ligase buffer (10x) | 1 µl | 1 µl |
| Plasmid backbone | ~ 300 ng | ~ 500 ng |
| Insert DNA | ~ 100 ng | ~ 100 ng |
| Water | Up to 10 µl | Up to 10 µl |
| **Total** | **10 µl** | **10 µl** |

**Transformations of calcium competent *E. coli* cells**

Aliquots of competent cells were thawed on ice until melted and split into 100 µl aliquots. SLiCE product (10 µl) or plasmid DNA (50 ng) was added to cells and left on ice for 20 min, then heat shocked in a water bath at 42 °C for 2 min and then placed back on ice for 2 min. 800 µl of L-broth was then added and cells were left to incubate at 37 °C for 90 min at 200 r.p.m agitation. These samples were then centrifuged at 11,000 x g for 1 min and 800 µl of supernatant was removed. The sample was resuspended in the remaining broth and plated on L-agar plates containing the antibiotic needed to maintain the plasmid. These were incubated overnight at 37 °C.

**Natural transformation of *A. baumannii***

A single colony was used to inoculate 2 ml of L-broth and grown to $OD_{600}$ = 1 , at 37 °C, 200 r.p.m agitation. This culture was diluted to $OD_{600}$= 0.01 in PBS by adding 2 µl of bacterial culture to 198 µl of PBS. 2.5 µl of this diluted culture was combined with 2.5 µl (~50 ng) of plasmid DNA and 2.5 µl of this was pierced into 1 ml of transformation media (2% Euromedex agarose D3 and 5 g/L tryptone) in an Eppendorf tube. This was incubated overnight at 37 °C. The next day 100 µl of PBS was added and vortexed. 20 µl was plated onto L-agar with antibiotics needed to maintain the plasmid and incubated overnight at 37 °C. Colonies were then patched onto fresh antibiotic L-agar plates for selection in colony PCR.

**Sanger sequencing**

Isolated plasmids to be sequenced were diluted in sterile water to concentrations required by sequencing providers. Plasmids were sent with primers listed in **Table 4** to Eurofins Sanger sequencing or Azenta Genewiz. Results were analysed using sequencing alignment tools on Benchling.

**Measurement of fluorescence**

To quantify the interaction between a sRNA and mRNA in *E. coli* and *A. baumannii,* the changes in fluorescence between strains containing the 2 plasmid systems were measured in a 96 well plate in a plate reader. Individual *E. coli* or *A. baumannii* colonies were used to inoculate 4 ml L-broth containing apramycin and tetracycline. 5 µl of overnight culture were inoculated into 1ml fresh L-broth containing apramycin and tetracycline and incubated at 37°C and 220 rpm agitation for 30 h. The cultures were then aliquoted into 96-well plates (Corning, Costar) and fluorescence (arbitrary units) and optical density at 600 nm ($OD_{600}$) were measured in a BioTek Synergy HTX Multimode Reader with excitation filter (485/20 nm) and emission filter (528/20 nm), gain 35. The fluorescence of strains was compared by quantifying the observed fluorescence relative to the $OD_{600}$. When comparing the mean values of 2 strains, an unpaired t-test was used, when comparing more than 2 strains, one way ANOVA with multiple comparisons, Tukey's test post hoc test was used. The sample fluorescence was divided by the control strain fluorescence to calculate the fold change. When measuring fluorescence over 30 h, overnight cultures were adjusted to an $OD_{600}$of 0.1 in PBS and 10 µl was inoculated into 96 well plate containing 100 µl of L-broth to a final $OD_{600}$of 0.01. The plate was incubated at 37 °C shaking in the Synergy H1™ Hybrid Multi-Mode microplate fluorometer (Bio-Tek) and $OD_{600}$ and fluorescence (excitation (485 nm) and emission (508 nm), gain 50) was measured every 15 mins for 30 h. Relative fluorescence was calculated by minusing the fluorescence blank and dividing by the $OD_{600}$ for each time point.

**Twitching motility assay**

*A. baumannii* strains were streaked on L-agar plates with apramycin and 20 colonies of similar size were stab inoculated into the centre of a motility plate (5% (w/v) agarose, 5 g/L tryptone and apramycin) using a toothpick. The plates were sealed in a bag and incubated in an upright position for 5 days at 37 °C. Interface motility zones were outlined and quantified using Image J imaging software. One way ANOVA with multiple comparisons, Tukey's test post hoc was performed to analyse the data.

**DNA uptake assay**

*A. baumannii* colonies were inoculated into L-broth (2 ml) with apramycin and grown at 37°C for 3 hours. Cultures were then adjusted to an $OD_{600}$ of 0.01 to ensure comparable cell densities. For transformations, 5 µl of the diluted bacterial culture was mixed with 20 ng of plasmid DNA. A 2.5 µl aliquot of this mixture was pierced onto transformation media and incubated overnight at 37°C. Following incubation, bacterial cells were resuspended in 100 µL PBS, serially diluted and plated onto L-agar plates with or without tetracycline and apramycin. Transformants were determined by calculating the proportion of tetracycline-resistant colonies relative to the total viable population.

**Whole cell lysate preparation**

To prepare *A. baumannii* AB5075 protein whole cell lysate, 4 ml of L-broth was inoculated and grown overnight. The next day the $OD_{600}$ was measured and adjusted to $OD_{600}$ 0.05 in L-broth. It was then centrifuged in 1.5 ml tubes at 2,500 x g for 5 mins at 4 °C. The pellets were washed and centrifuged at 2,500 x g for 5 mins at 4 °C twice in PBS. The pellets were resuspended in 25 µl 2 x Lämmli buffer (0.5 M Tris- HCl pH 6.8, 15% (w/v) SDS, 80% (v/v) glycerol, 1% (w/v) bromophenol blue, 200 mM dithiothreitol) and 25 µl PBS and then heated for 10 mins at 95 °C. These were centrifuged at 21,000 x g at 4 °C for 1 min. These whole cell lysates were stored at -20 °C for later use.

**SDS PAGE and Western blotting**

Whole cell lysates were separated into proteins by Sodium Dodecyl Sulfate Polyacrylamide Gel Electrophoresis (SDS PAGE). The gel was composed of a 12.5% separating gel (40% acrylamide bisacylamide, 1.5M Tris HCl pH 8.8, 15% SDS, 99% glycerol, water, Tetramethylethylenediamine (TEMED), 10% APS) and 6.6% stacking gel (40% acrylamide bisacylamide, 0.5M Tris HCl pH 6.8, 15% SDS, water, TEMED, 10% APS). The whole cell lysate samples were boiled again and spun at max speed for 1 min. 15 µl of sample was loaded into each lane and 5 µl of EZ-Run™ Prestained Rec Protein Ladder (Fisher Scientific) as a size comparison. The gel was run at 100 V for 2-3 h in 1x

SDS running buffer (0.1% v/v SDS, 192mM glycine, 25mM tris, water). The gel was then washed with deionised water and soaked in 1x transfer buffer (25 mM Tris, 0.19 M glycine) for 10 min. 3 mm filter paper (Whatman) and 0.45 µm AmershamTM Protran® nitrocellulose membranes (Merck) were also soaked in 1x transfer buffer for 10 min. These parts were then assembled into a "sandwich" in gel holder cassettes and placed in the Mini Trans-Blot Electrophoretic Transfer Cell (Bio-Rad) with an ice pack to prevent protein degradation. The proteins were blotted onto the membrane at 300mA for 90 min. To confirm even transfer of protein. Ponceau S (Sigma) was used to stain the membrane and then washed off with water. The membranes were then blocked overnight at 4 °C in blocking buffer (5% (w/v) skimmed milk powder, 0.9% (w/v) NaCl and 10 mM Tris/HCl pH 7.5). The membranes were then washed for 15 mins twice in antibody buffer (0.5% (w/v) skimmed milk powder, 0.9% (w/v) NaCl, 0.1% (v/v) Tween-20 and 10 mM Tris/HCl pH 7.5). The membranes were then washed in antibody buffer containing anti-DnaK (*E. coli*, Enzo), diluted 1:5,000 and anti-GFP (Proteintech) diluted 1:10,000 for 1 h at room temperature. Subsequently, the membrane was washed 4 times for 10 mins in PBST (PBS and 0.05 % (v/v) Tween-20). Then the membrane was washed in antibody wash containing the secondary antibody anti-mouse IgG (H+L) horseradish peroxidase (HRP) diluted 1:10,000 (Milipore) for 90 min. The membrane was then washed 3 times for 10 min each in PBST. Directly before imaging the membrane was flooded with ECL chemiluminescent HRP substrate. The chemiluminescent signal was visualised using the ImageQuant LAS4000 (GE Healthcare). Western blot bands were quantified using ImageJ. Area under the curve graphs were made for each sample and DnaK band. The sample values were divided by the DnaK value to get the value relative to DnaK. These values were plotted and a one way ANOVA with multiple comparisons, Tukey's test post hoc was performed. To calculate the fold change in band intensity of samples in relation to the control, the band intensities values were averaged and the control was divided by the respective sample.

**Antibiotic disc diffusion assay**

*A. baumannii* strains were grown overnight in Mueller Hinton Broth at 37 °C and adjusted to McFarland standard 0.5 (equivalent $OD_{600}$ = 0.08 - 0.1) in sterile PBS. A sterile cotton swab was soaked into the inoculum and rotated along the edge of the tube to

ensure equal amount of inoculum for each sample. The swab was lawned over an Mueller Hinton agar plate in 3 directions to ensure equal coverage of entire plate. An antibiotic disc dispenser was used to dispense the antibiotics. The plates were incubated for 16-18 h at 37 °C and zone of inhibition was measured in mm using a ruler. Results were interpreted using Clinical and Laboratory Standards Institute disk diffusion guidelines (CLSI M100 ED35:2025).

# Chapter 1 Results

## Functional characterisation of Arp

109 Arp-*pilA* chimeric reads were revealed from Hi-GRIL-seq analysis with 88% of these mapping to a interaction duplex at the 5' UTR of *pilA*, sequestering its Shine Dalgarno (SD) sequence (Hamrock *et al.*, 2024). This suggests that Arp is post-transcriptional repressor of PilA. As *pilA* encodes the principal subunit for T4P, Arp has been proposed to regulate T4P-mediated activities such as twitching motility and DNA uptake.

## Fluorescence-based reporter system validates Arp-*pilA* translational repression in *E. coli* TOP10 and *A. baumannii* AB5075

Previously, the Arp-*pilA* interaction had been confirmed bioinformatically and *in vivo* in *E. coli* using the existing $pP_L$ and pXG10 fluorescence-based reporter system by Fergal Hamrock in the Kröger lab **(Figure 2)**. To validate the sRNA-mRNA interaction in *A.baumannii* AB5075, a new two plasmid fluorescence based reporter system was employed. The recently created pAMCK reporter system has the same function as the historical $pP_L$, pXG10 plasmids but can replicate in both *E. coli* and *A. baumannii* (Mogre *et al.*, 2025). The plasmids contain compatible origins of replication pWH1266 and pRSF1010, constitutive promoters $P_{LtetO}$ and $P_{LlacO}$ and a truncated sfGFP to create translational fusions. The plasmid pAMCK14 expresses the sRNA of interest and has apramycin resistance **(Figure 3 A).** The plasmid pAMCK15 expresses a control nonsense sRNA, and also an apramycin resistance gene **(Figure 3 B).** Both pAMCK14 and pAMCK15 contain the $P_{LlacO}$ promoter and *rrnBT1* terminator. pAMCK18 expresses the target mRNA translationally fused to sfGFP from the $P_{LtetO}$ promoter and has the same terminator and a tetracycline resistance gene **(Figure 3 C).** If cells harbouring pAMCK14-sRNA and pAMCK18-mRNA show a change in fluorescence levels compared to the control (pAMCK15), it would suggest the sRNA influences the translation of the target mRNA.

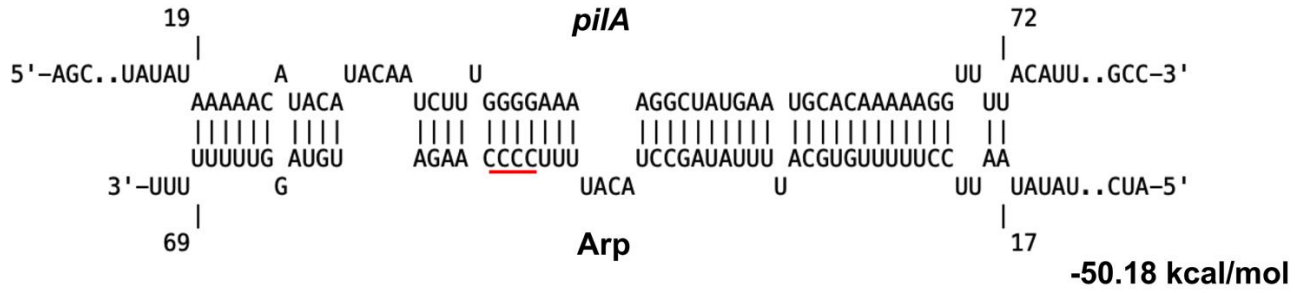


**Figure 2: Arp-*pilA* base pair interaction predicted by IntaRNA (Busch *et al.*, 2008).** Arp predicted interacting region highlighted in red. The interaction has a highly negative hybridisation energy (-50.18 kcal/mol), suggesting strong base pairing between Arp and *pilA*.

To create the new plasmid-system, plasmid backbone PCR was carried out to amplify linearised pAMCK14 and pAMCK18 plasmids. The sRNA Arp and the mRNA *pilA* were PCR amplified from *A. baumannii* AB5075 genomic DNA with primers which add SLiCE sequences. The sRNA primer added 100 base pairs downstream of the gene to ensure termination. To investigate the importance of the predicted four-cytosine nucleotide interaction region **(Figure 2),** an Arp* variant was generated in which these nucleotides were substituted with four guanines. Similarly, a PilA* construct was created with compensatory mutations, replacing four guanines with cytosines. If Arp* exhibits fluorescence levels similar to the control, this would suggest that the mutated region is critical for initiating the interaction between the sRNA and mRNA. Subsequently, if PilA* restores fluorescence to wild-type Arp levels, it would further confirm the significance of this interaction region.

In *E. coli*, pAMCK18-pilA expressing cells fluoresced green when streaked on L-agar, showing sfGFP was successfully being translated. Expression of Arp from pAMCK14-Arp reduced the appearance of green fluorescence, and pAMCK15 caused no reduction in fluorescence suggesting Arp was post-transcriptionally regulating PilA-sfGFP translation. The plasmid expressing the mutated Arp* (pAMCK14-Arp*) showed less reduction in fluorescence compared to wild-type Arp. To investigate this interaction in the native bacteria, this was replicated in *A. baumannii* AB5075 Δ*arp* via natural transformation and the same results were recapitulated **(Figure 3 D).** Strains containing pAMCK18-PilA* showed no fluorescence as the compensatory mutation disrupts the Shine Dalgarno (SD)

sequence, preventing the sfGFP from being translated, therefore these strains were not imaged.

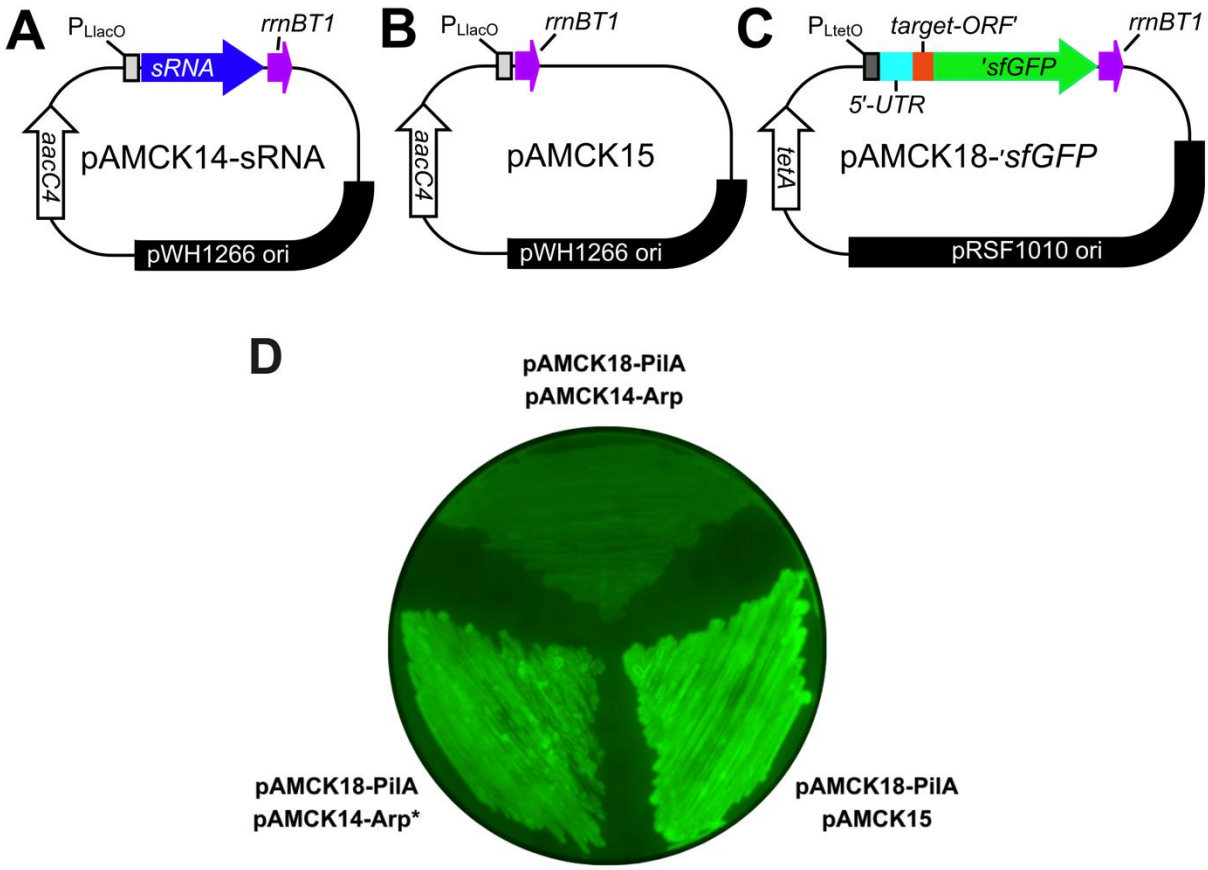


**Figure 3: Schematic plasmid maps of pAMCK 2 plasmid system including (A) pAMCK14, (B) pAMCK15 and (C) pAMCK18 (Mogre *et al.*, 2025).** (A) pAMCK14 expresses a small RNA from the $P_{LlacO}$ promoter and has the rrnBT1 terminator. (B) pAMCK15 expresses a small nonsense RNA contains the same promoter and terminator as pAMCK14. Both these plasmids also have the pWH1266 origin of replication and the *aacC4* gene which confers apramycin resistance. (C) pACMK18 expresses a translational fusion of a target gene to sfGFP lacking a start codon. This plasmid contains the $P_{LtetO}$ promoter, the rrnTB1 terminator, the pRSF1010 origin of replication and the *tetA* gene conferring tetracycline resistance. (D) Arp inhibits PilA-sfGFP translation in *A. baumannii* AB5075 *Δarp.* Overexpression of Arp reduces PilA-sfGFP expression by visual quantification on a plate. PilA-sfGFP translation is not impacted by overexpression of the nonsense sRNA on pAMCK15. PilA-sfGFP expression is slightly reduced by overexpression of mutant Arp*. PilA-sfGFP expression is reduced by overexpression of Arp. Imaged on the ImageQuant LAS4000 (GE Healthcare).

**Quantification of Arp-PilA interaction *in vivo* in *E. coli* TOP10 and *A. baumannii* AB5075**

The strains used for visual quantification of the sRNA mRNA interaction, pAMCK18-PilA transformed with either the Arp overexpression plasmid (pAMCK14-Arp, pAMCK14-Arp*) or the control sRNA plasmid (pAMCK15) were then used for quantification of the change in fluorescence after 30 h in both *E. coli* TOP10 and *A. baumannii* AB5075 *Δarp*. In both *E. coli* and *A. baumannii* AB5075 *Δarp*, Arp overexpression significantly reduced PilA-sfGFP fluorescence (~1.3-fold, $p < 0.01$ and 1.9-fold, $p < 0.001$ respectively) compared to the control strain **(Figure 4 A,B)**. In *A. baumannii* AB5075 *Δarp* the repression was relieved by the mutation of the Arp seed region (Arp*), restoring fluorescence to wild-type levels **(Figure 4 B)**. The overexpression of Arp* has significantly higher fluorescence compared to the overexpression of Arp ($p < 0.001$) in *A. baumannii* AB5075 *Δarp.* PilA* mutation shows no fluorescence due to disruption of SD sequence.

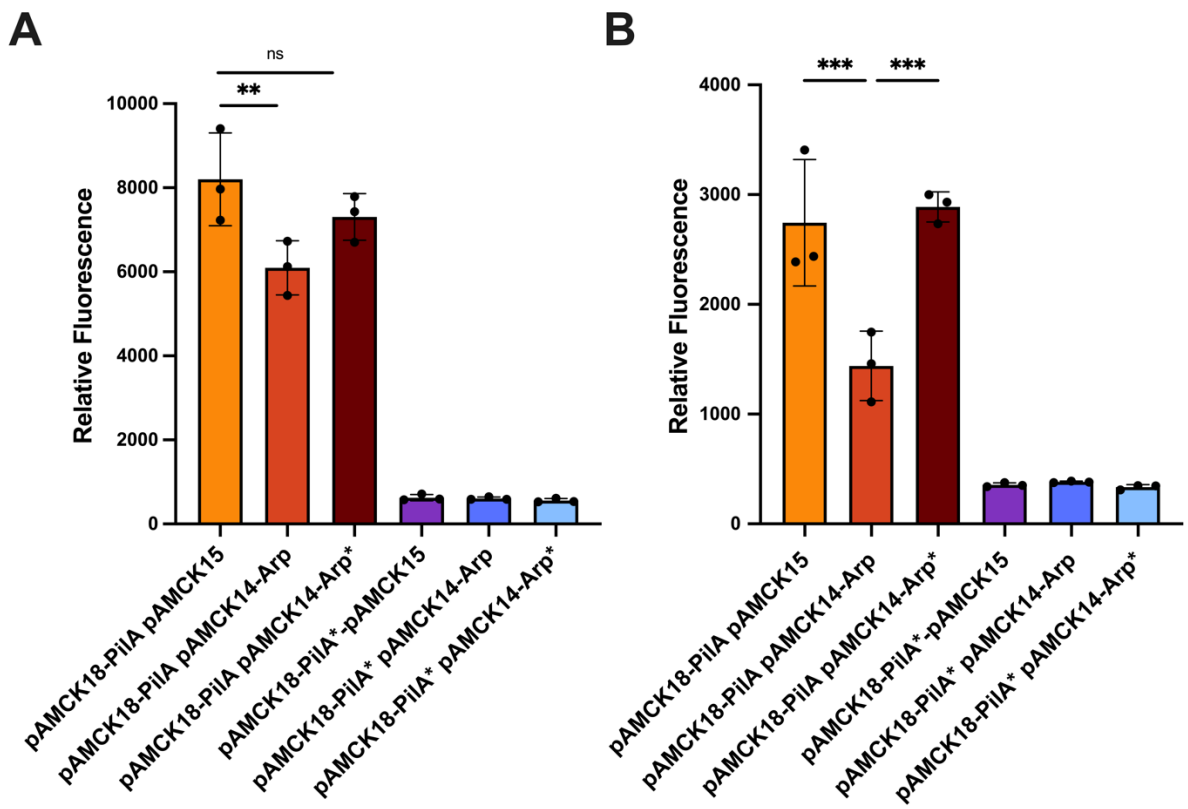


**Figure 4: Arp inhibits PilA-sfGFP translation. Overexpression of Arp reduces PilA-sfGFP expression *in vivo* in both (A) *E. coli* TOP10 and (B) *A. baumannii* AB5075 *Δarp*, measured by PilA-sfGFP translational reporters**. Error bars represent the standard deviation of three independent biological replicates (n=3). Statistical analysis was performed using one-way ANOVA with Tukey's post hoc test. Significance was

defined where * denotes $P<0.05$, ** denotes $P<0.01$, *** denotes $P<0.001$ and **** denotes $P<0.0001$.

**Arp downregulates PilA, restricting twitching motility in *A. baumannii* AB5075**

Twitching motility in *A. baumannii* is a T4P meditated movement, and therefore involves PilA, an essential component of T4P (Harding *et al.*, 2013, Craig *et al.*, 2019, Salinas *et al.*, 2025, Harding Christian *et al.*, 2013). As Arp has been shown to downregulate PilA, it was investigated if this had an effect on twitching motility. The non-motile *pilA* deletion strain was used as a negative control (*ΔpilA)*. The wild-type *A. baumannii* AB5075 carrying the control plasmid pAMCK15 was compared to *A. baumannii* AB5075 *Δarp* carrying either the control plasmid (pAMCK15) or the overexpression of Arp or Arp* plasmid (pAMCK14-Arp and pAMCK14-Arp*) **(Figure 5 A).** Briefly, 20 colonies of equal size were individually stab inoculated into motility plates and incubated for 5 days at 37°C. The resulting twitching motility zones were measured and compared **(Figure 5, A B).** Arp appears to reduce twitching motility as the Arp deletion strain showed a significant increase in twitching motility compared to wild-type ($p < 0.0001$) **(Figure 5 B)**. The strains containing a plasmid overexpressing Arp showed significantly reduced motility compared to wild-type and *Δarp* ($p < 0.001$ and $p < 0.0001$ respectively) **(Figure 5 B)**. The reduction of motility by Arp overexpression is similar to *ΔpilA* levels. The overexpression of Arp* with a mutated interacting region significantly increased twitching motility compared to wild-type and Arp overexpression ($p <0.001$ and $p < 0.0001$ respectively), showing the importance of this interacting region in the control of Arp over *pilA* mRNA.

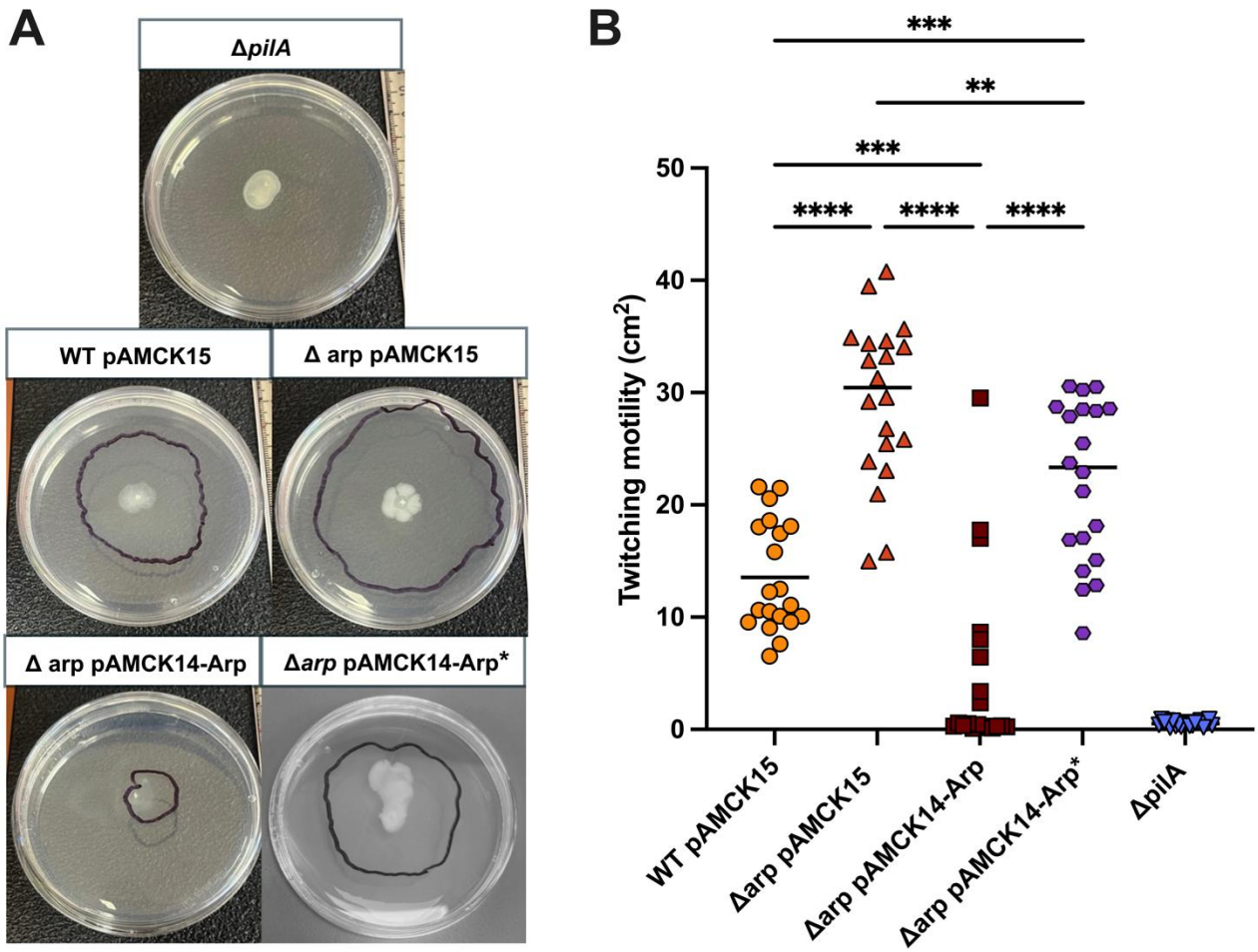


**Figure 5: Arp regulates twitching motility in *A. baumannii* AB5075. (A) representative images of twitching motility plates and (B) quantification of zones of motility in** *A. baumannii* AB5075 wild-type (WT) and Arp-deletion strains (Δ*arp*) carrying either an empty vector (pAMCK15), an Arp overexpression plasmid (pAMCK14-Arp), or an interacting region mutant of Arp (pAMCK14-Arp*)**.** A Δ*pilA* strain was included as a negative control. Error bars represent the standard deviation of twenty independent biological replicates (n=20) and statistical analysis was performed using one-way ANOVA with Tukey's post hoc test. Significance was defined where * denotes $P<0.05$, ** denotes $P<0.01$, *** denotes $P<0.001$ and **** denotes $P<0.0001$.

**Arp downregulates DNA uptake in *A. baumannii* AB5075**

The ability of Arp to modulate natural transformation in *A. baumannii* was assessed next via DNA uptake assay. The ability of each strain to uptake plasmid DNA (pAMCK18-PilA) overnight in transformation media was assessed. The transformation frequency was determined by plating on selective and non-selective agar. Strains which grew on tetracycline and apramycin plates had successfully obtained the plasmid DNA. To confirm comparable levels of growth between strains, colony forming units per ml (CFU/ml) was determined on non-selective agar and no significant difference between colony counts was determined **(Figure 6 A).** The Arp deletion strain *Δarp* with control pAMCK15 plasmid showed no difference in DNA uptake ability compared to wild-type ($p < 0.0001$) **(Figure 6 B).** However, there was a complete lack of DNA uptake in the Arp overexpression strain in comparison to wild-type ($p < 0.0001$) **(Figure 6 B).** The overexpression of seed region mutated Arp (pAMCK14-Arp*) partially restores DNA uptake suggesting other components of the sRNA still have binding capacity with *pilA* mRNA. These results suggest that the repression of *pilA* translation by Arp, impacts the DNA uptake machinery inhibiting natural transformation.

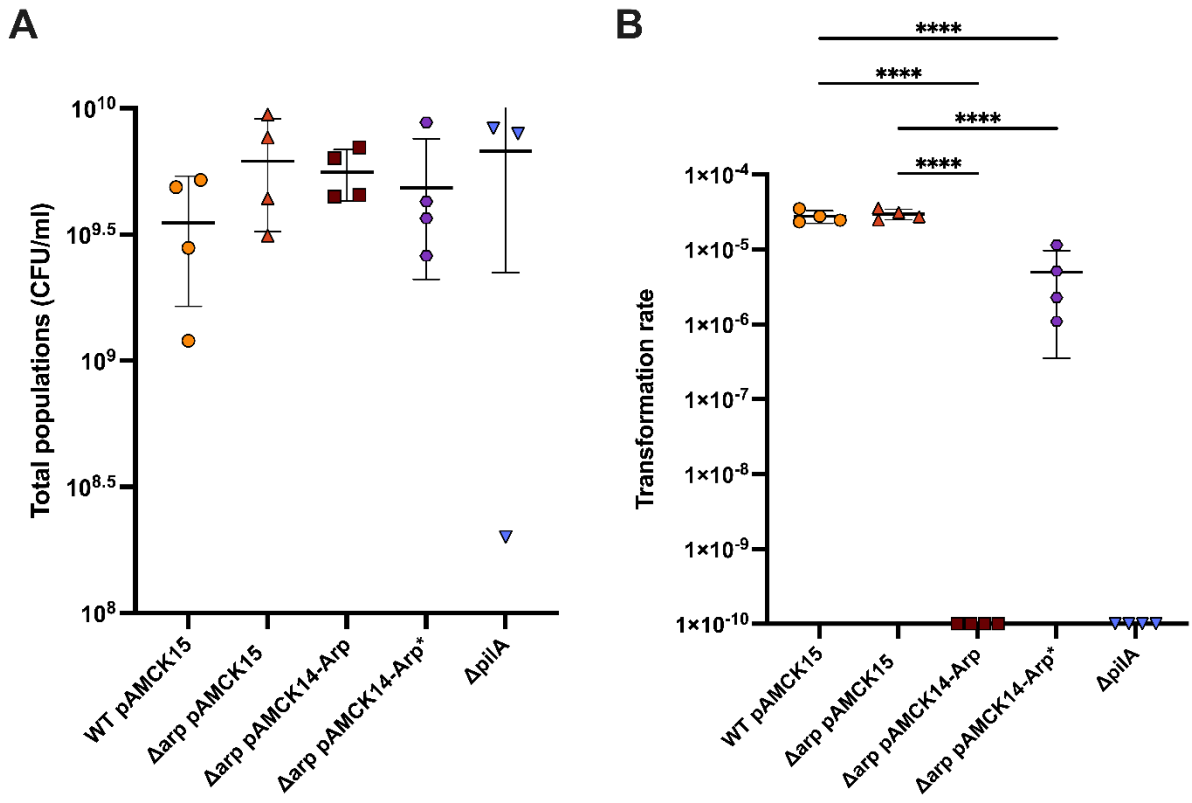


**Figure 6: Arp regulates natural transformation in *A. baumannii*.** (A) Total populations (CFU/ml) of *A. baumannii* AB5075 wild-type (WT) and Arp-deletion strains (Δ*arp*) carrying either an empty vector (pAMCK15), an Arp overexpression plasmid

(pAMCK14-Arp), or a interacting region mutant of Arp (pAMCK14-Arp*). A Δ*pilA* strain was included as a negative control. (B) natural transformation frequencies of the same strains. Error bars represent standard deviation of four independent biological replicates (n=4). Statistical analysis was performed using one-way ANOVA with Tukey's post hoc test. Significance was defined where * denotes $P<0.05$, ** denotes $P<0.01$, *** denotes $P<0.001$ and **** denotes $P<0.0001$.

# Chapter 2 Results

## Programmable sRNA to re-sensitise *A. baumannii* to carbapenems

To investigate the potential therapeutic functions of ASOs, the new plasmid system pAMCK can aid in the development of synthetic programmable sRNAs in *A. baumannii* similar to toolboxes created for *E. coli* (Brück *et al.*, 2024, Köbel *et al.*, 2022). Identifying and understanding the mechanisms of natural antisense RNA in bacteria such as sRNA is crucial for understanding the theory for the development of synthetic ASO therapies. Based on natural *trans*-sRNAs, synthetic programmable sRNAs are composed of a scaffold sRNA, mRNA binding region and termination loop.

This study proposes a method of creating synthetic programmable sRNA therapeutics using the new pAMCK plasmid system in *A. baumannii.* The programmed sRNA was designed by taking a known sRNA and creating an altered "seed" region which binds the target transcript and measuring the effect in *A. baumannii* **(Figure 7).** Due to the rise of CRAb and the need for new treatments for this resistant strain, the carbapenemase gene Oxa-23 was chosen as the target of the programmable sRNA. The synthetic downregulation of this antibiotic resistance determinant aimed to re-sensitise *A. baumannii* to already available carbapenem antibiotics.

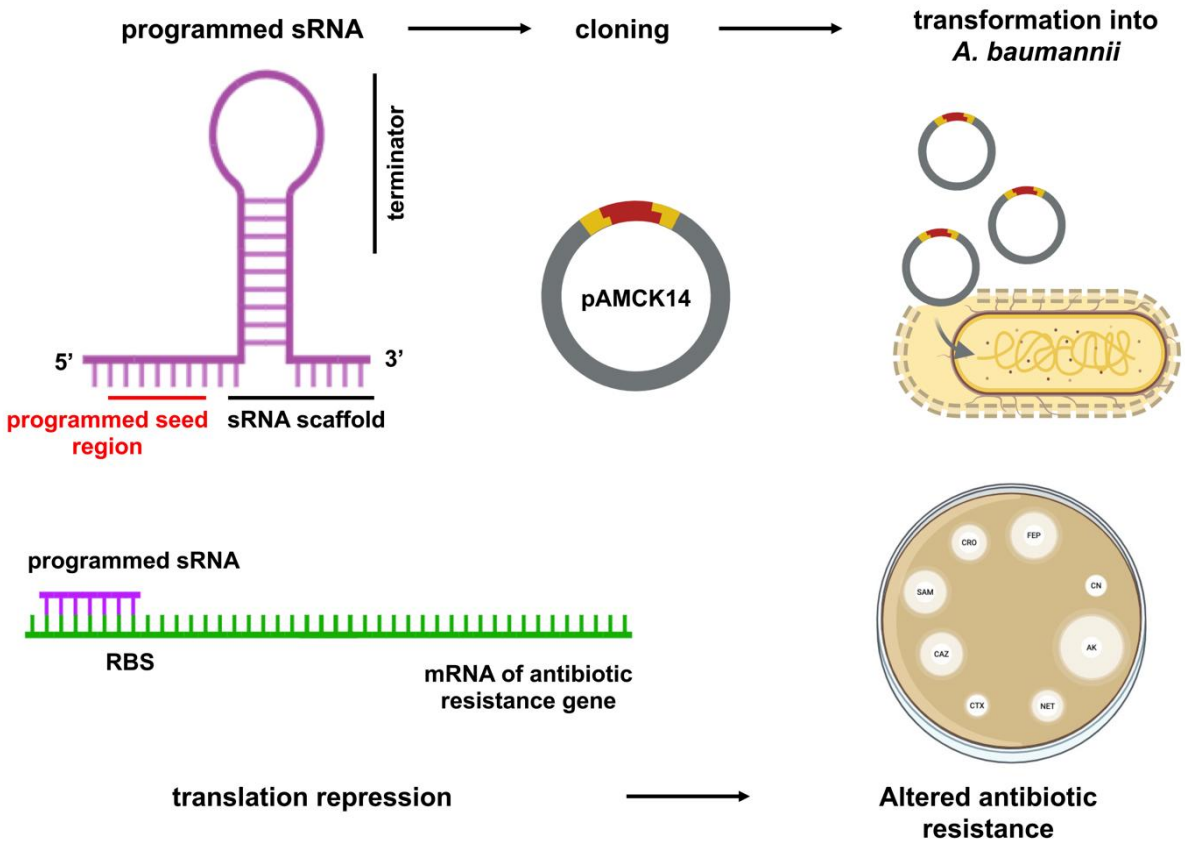


**Figure 7**: **Overview of programmable sRNA workflow.** Programmable sRNAs are created with an sRNA scaffold, seed region which binds the target mRNA and terminator region. The sRNA is cloned into pAMCK in *E. coli* and then transformed into *A. baumannii* AB5075, where it represses the target gene, inducing a phenotype of less fitness, such as reduced antibiotic resistance.

### Determining suitable sRNA scaffold for programmable sRNA

Programmable sRNAs are potential therapeutics based off natural bacterial sRNA. These RNA-based antibiotics can be programmed to target essential genes in pathogenic bacteria killing them or altering the targeted pathway (Vogel, 2020). Programmable sRNA consist of two components, the scaffold sequence and the target binding sequence. A reporter system is also needed to investigate the effectiveness of the programmed sRNA. Previous plasmid toolkits for generating synthetic sRNA have been described in other bacteria but not *A. baumannii* (Köbel *et al.*, 2022). As the pAMCK plasmid system has been proven to be efficient for investigating sRNA-mRNA interactions in *A. baumannii* (Mogre *et al.*, 2025), it was chosen as a plasmid toolkit for the generation and assessment of synthetic sRNA **(Figure 7)**. To build a programmable sRNA, two previously described sRNAs were investigated as potential sRNA scaffolds, *Salmonella enterica* serovar

Typhimurium sRNA RyhB-2 which binds to *sodB* mRNA and *Acinetobacter baumannii* sRNA Aar which binds to *carO* mRNA (Troxell *et al.*, 2011, Calderón *et al.*, 2014, Hamrock *et al.*, 2024). The level of repression of target mRNA fluorescence was measured for both sRNAs in the same way as described in chapter 1.

**Quantification of sRNA scaffold interaction with known mRNA targets in *E. coli* and *A .baumannii* AB5075**

To investigate the interactions of RyhB-2 with *sodB*, pACMK18-sodB was created with sodB translationally fused to sfGFP aswell as the sRNA overexpression plasmid pAMCK14-RyhB-2. Similarly for Aar with *carO*, pAMCK18-CarO was created with the translational fusion of *carO* to sfGFP and pAMCK14-Aar overexpressed Aar. In both *E. coli* TOP10 and *A. baumannii* AB5075, pAMCK18-sodB was co-tranformed with either the control sRNA plasmid (pAMCK15) or the sRNA overexpression plasmid (pAMCK14-RyhB-2). Similarly in both *E. coli* TOP10 and *A. baumannii* AB5075 *Δaar* pAMCK18-CarO was co-transformed with either the control plasmid (pAMCK15) or the overexpression plasmid (pAMCK14-Aar).

In *E. coli,* RyhB-2 overexpression significantly reduced SodB-sfGFP fluorescence (~11-fold, $p < 0.0001$) and Aar overexpression significnatly reduced CarO-sfGFP fluorescence (~2.7-fold, $p < 0.0001$) **(Figure 8 A,B).** In *A. baummannii* AB5075 wild-type, RyhB-2 overexpression had no significant effect on SodB-sfGFP fluorescence (~1-fold, $p > 0.05$) **(Figure 8 C).** In *A. baumannii* AB5075 *Δaar,* Aar overexpression significnatly reduced CarO-sfGFP fluorescence (~1.2-fold, $p < 0.05$)**(Figure 8 D).**

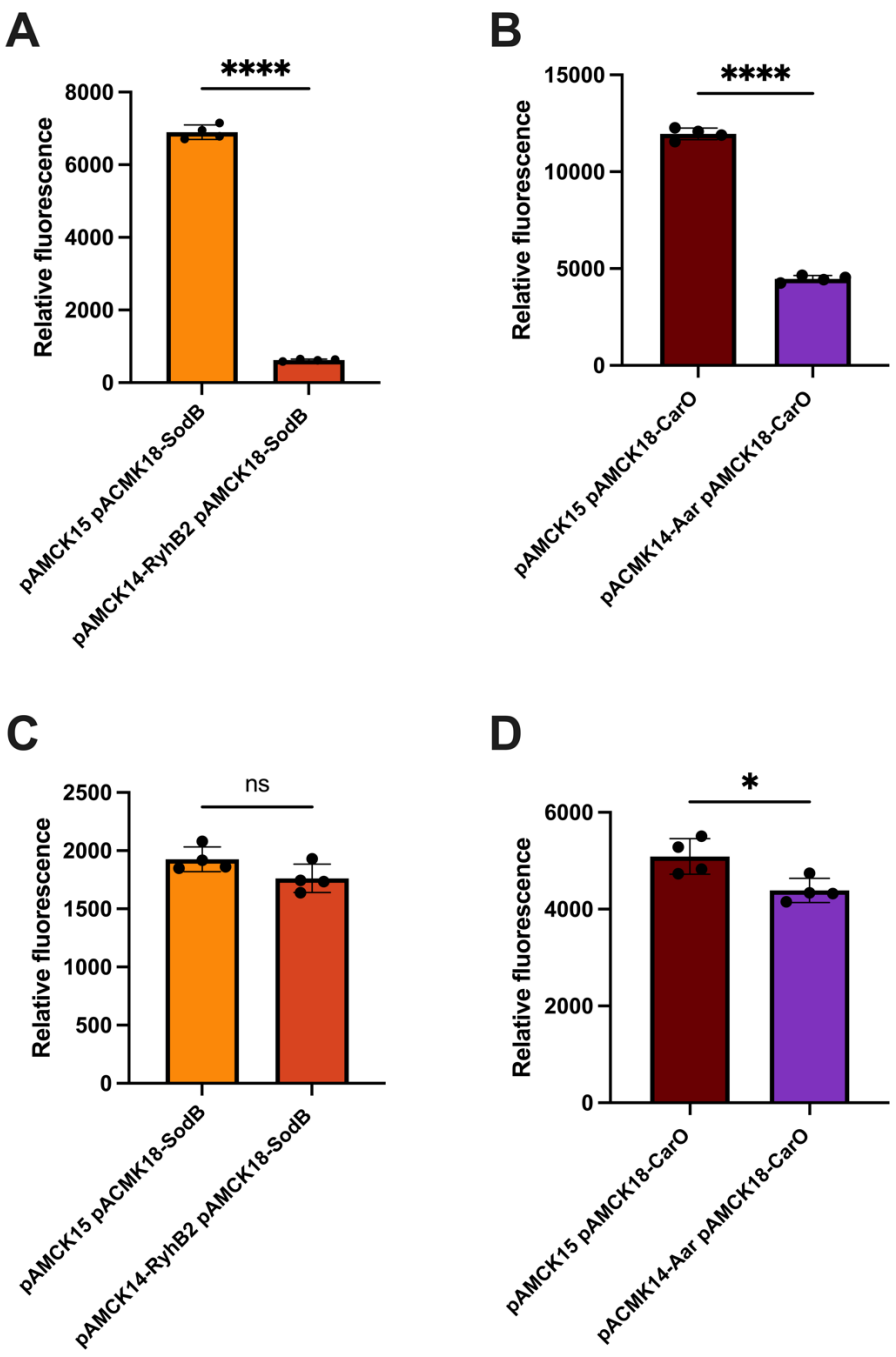


**Figure 8: RyhB-2 overexpression inhibits SodB-sfGFP translation *in vivo* in (A) *E. coli* but not (C) *A. baumannii*. Aar overexpression inhibits CarO-sfGFP translation in (B) *E. coli* and (D) *A. baumannii* AB5075 *Δaar*, measured by translational reporters**. Error bars represent the standard deviation of four independent biological replicates (n=4). Statistical analysis was performed using unpaired T test. Significance was defined where * denotes $P<0.05$, ** denotes $P<0.01$, *** denotes $P<0.001$ and **** denotes $P<0.0001$.

**Verifying optimal time to measure fluorescence in *A. baumannii* AB5075**

To investigate if there was a time-dependent effect on the interactions between RyhB-2 with SodB and Aar with CarO, a 30 h fluorescence growth experiment was performed on these *A. baumannii* AB5075 strains measuring fluorescence at constant intervals. The optical density at 600nm ($OD_{600}$) and fluoresence (arbitrary units) was measured every 15 min over a 30 h period. Each strain showed typical growth dynamics showing a lag, log and stationary phase **(Figure 9 A,B).** Fluorescence (AU) appeared to increase with time for each strain, reaching its peak at 30 h **(Figure 9 C,D).** Relative fluorescence (AU/ $OD_{600}$) is also at its peak after 30 h for all strains **(Figure 9 E,F).** In *A. baumannii* AB5075, overexpression of RyhB-2 has no effect on the relative fluorescence of SodB-sfGFP **(Figure 9 E).** In *A. baumannii* AB5075 *Δaar,* the overexpression of Aar repressed the fluorescence of CarO-sfGFP (**Figure 9 F**). From this graph, endpoint relative fluorescence values were taken and plotted **(Figure 10).** Confirming the results from Figure 8 C, overexpression of RyhB-2 had no effect on the relative fluorescence of SodB-sfGFP ($p > 0.05$ )(**Figure 10 A).** Overexpression of Aar was found again to cause a significnat reduction on the fluorescence of CarO-sfGFP (~1.4-fold, $p < 0.01$)(**Figure 10 B).**

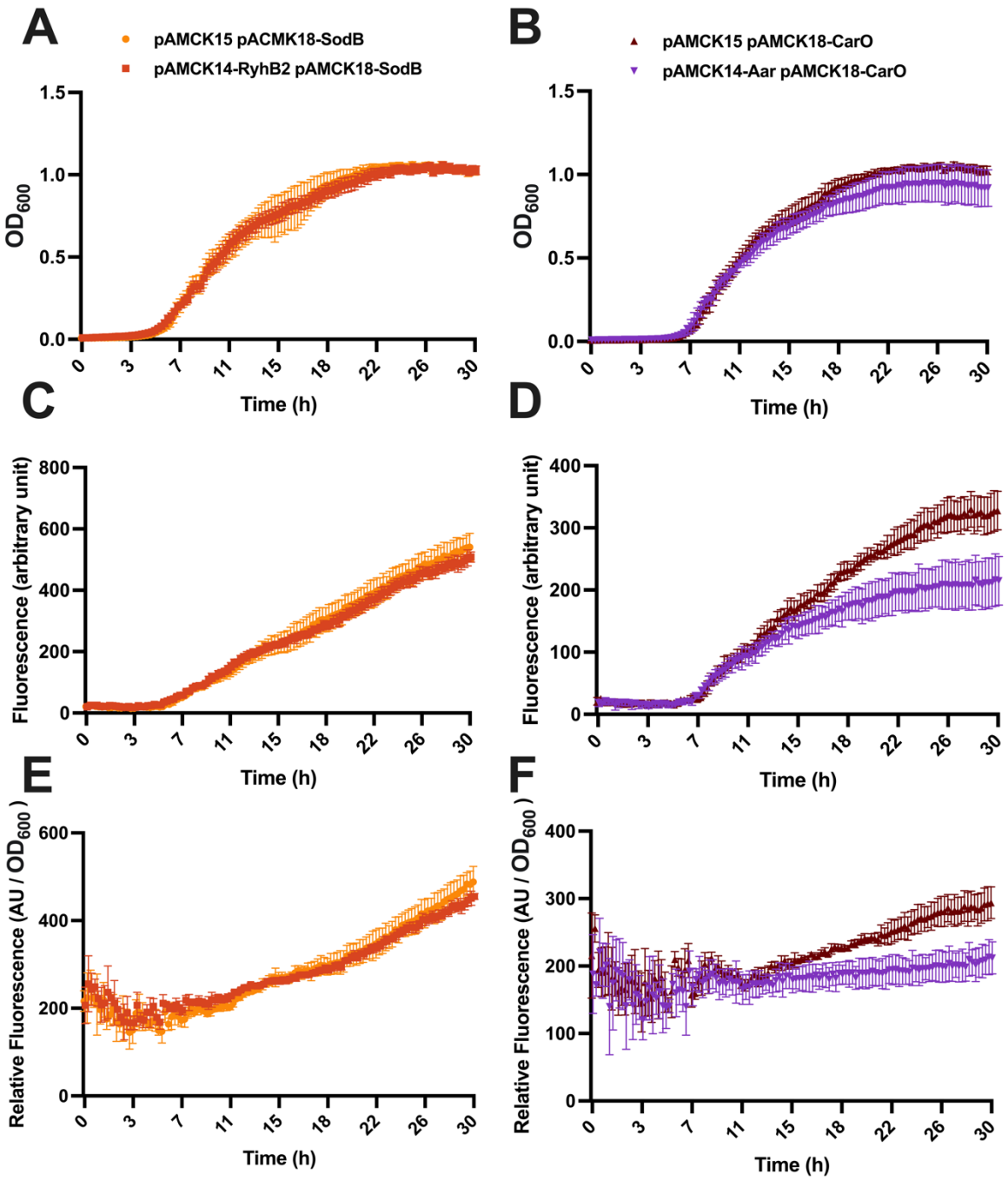


**Figure 9: Optimal time for measurement of relative fluorescence in *A. baumannii* AB5075 is 30 h.** Growth ($OD_{600}$) of *A.baumannii* AB5075 pAMCK18-SodB with control vector pAMCK15 or RyhB-2 overexpression **(A)** and *A. baumannii* AB5075 *Δaar* with pAMCK18-CarO with either control sRNA or Aar overexpression **(B)** over 30 hours. Fluorescence measurement (AU) of same strains over 30 hours. **(C,D)** Abundance of SodB-sfGFP (AU / $OD_{600}$ ) with overexpression of control sRNA compared to overexpression of Ryhb-2 does not change over 30 h **(E)** Overexpression of Aar reduces CarO-sfGFP abundance over 30 h **(F).** Four biological replicates are averages of three technical replicates (n=4).

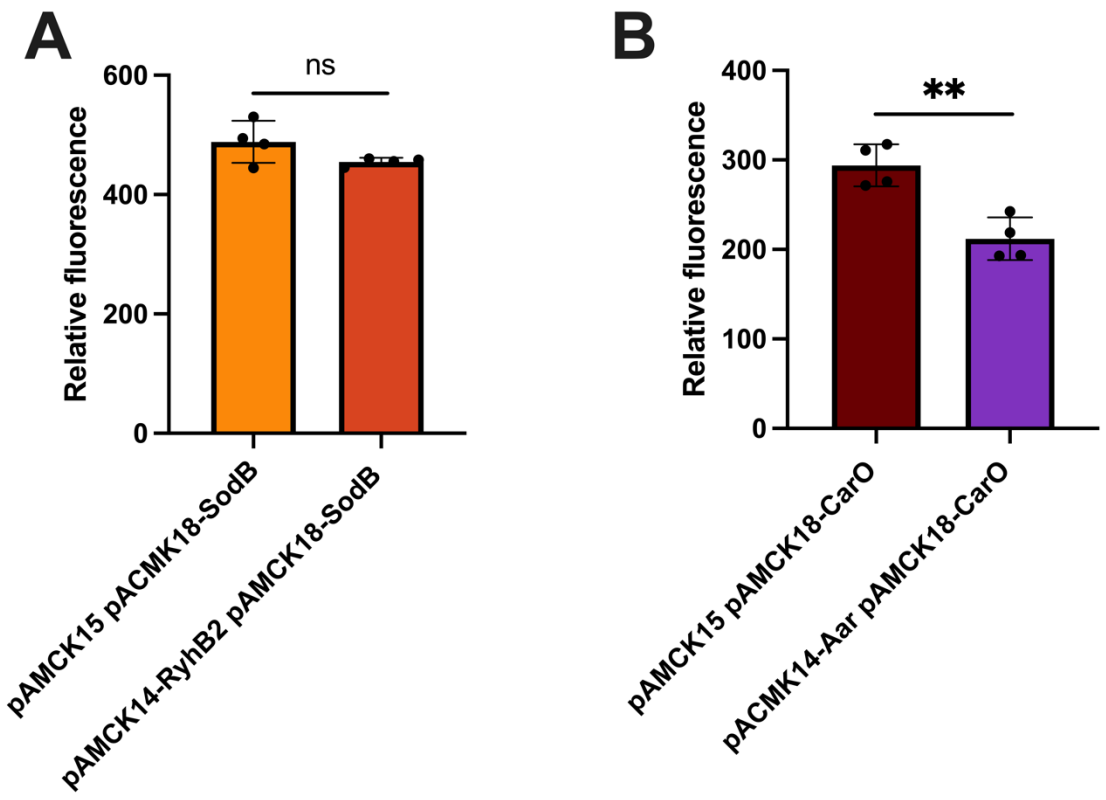


**Figure 10: RyhB-2 does not inhibit SodB translation in *A. baumannii* AB5075 (A), Aar inhibits CarO translation in *A. baumannii* AB5075 *Δaar* (B).** Data points taken from hour 30 of growth curve. Error bars represent the standard deviation of four independent biological replicates (n=4). Statistical analysis was performed using unpaired T test. Significance was defined where * denotes $P<0.05$, ** denotes $P<0.01$, *** denotes $P<0.001$ and **** denotes $P<0.0001$.

**Creation of the programmed sRNA Aar-oxa23 to target Oxa-23**

The fluorescence reporter system for Aar and CarO had a significant change in fluorescence in both *E. coli* and *A. baumannii,* unlike with RyhB-2 and SodB **(Figure 10).** Consequently, Aar was selected as the scaffold sRNA for the creation of a programmable sRNA system. To design an sRNA capable of downregulating an antibiotic resistance determinant in CRAb, a target involved in antibiotic resistance needed to be identified. The carbapenemase Oxa-23 was chosen as the target, as this encodes a key beta-lactamase contributing to carbapenem resistance in *A. baumannii.*

To create the system, plasmid backbone PCR was carried out to amplify linearised pAMCK14 and pAMCK18 plasmids. The 5'-UTR and the sequence encoding the first 30 amino acids of the *oxa-23* mRNA was PCR amplified from *A. baumannii* AB5075 genomic DNA with primers which add SLiCE sequences for pAMCK18. To amplify the programmed sRNA, primers were created which amplify the transcriptional start site of Aar including the altered programmable "seed" region and the SLiCE sequences. The seed region was determined by comparing the interaction of Aar with *carO* mRNA **(Figure 11 A).** The altered seed region consists of 12 nucleotides which have complementarity to the ribosome binding site (RBS) of Oxa-23 **(Figure 11 B, D).** The RBS was determined as the nucleotides starting 3 base pairs upstream of the start codon. The sRNA primer added SLiCE sequences and 100 base pairs downstream of the Aar gene to ensure termination. The programmed sRNA was named Aar-oxa23.

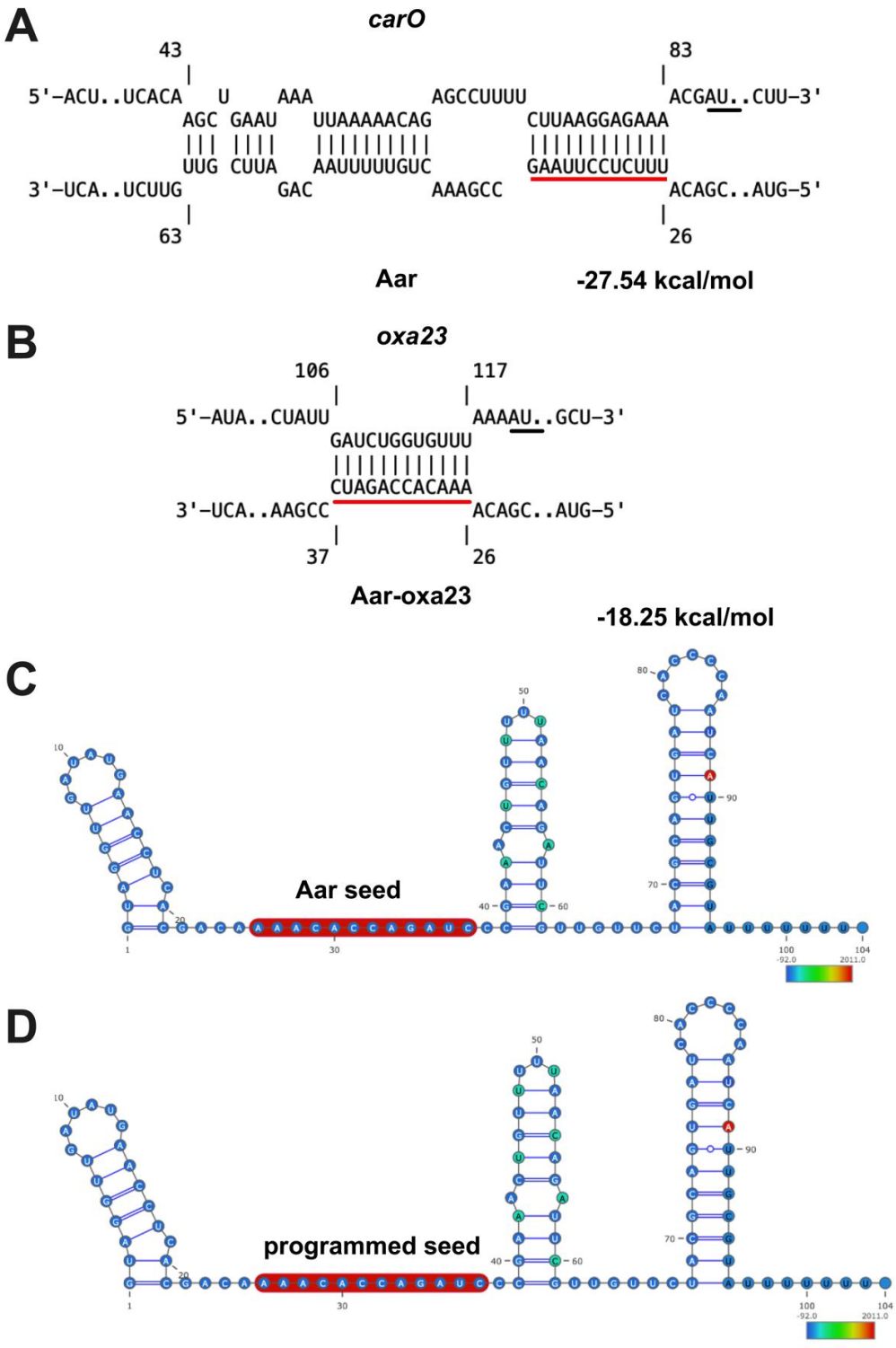


**Figure 11: Predicted interaction using IntaRNA of (A) Aar and *carO*, (B) Aar-oxa23 and *oxa-23*.** Underlined in red is the region where the nucleotides where changed, underlined in black is the start codon. The hybridization energy is noted. **The minimum free energy Aar (C) secondary structure and Aar-oxa23 (D) was predicted by RNAfold and represented with VARNA** (Darty et al., 2009; Lorenz et al., 2011). The colours of the nucleotides correspond to base-pairing probabilities and the seed region is highlighted.

**Programmed sRNA Aar-oxa23 represses translation of *oxa-23 in vivo* in *E. coli***

In *E. coli*, pAMCK18-oxa23 expressing cells were co-transformed with pAMCK15, pAMCK14-Aar or pAMCK14-Aar-oxa23 and streaked on L-agar with antibiotics. Overexpression of Aar-oxa23 caused a large reduction in fluorescence, while pAMCK15 caused no reduction in fluorescence. Overexpression of Aar caused a slight reduction in fluorescence **(Figure 12)**.

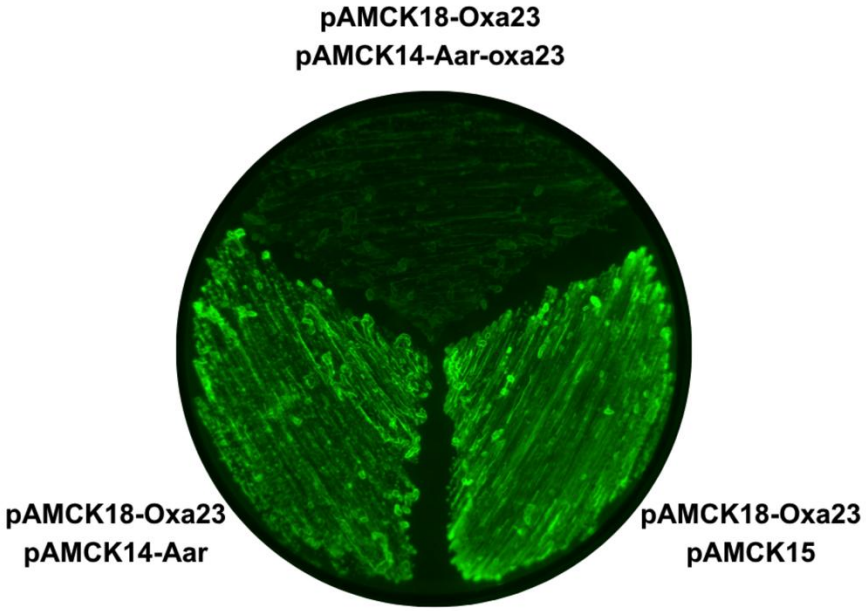


**Figure 12: Programmed sRNA Aar-oxa23 inhibits Oxa23-sfGFP translation in *E. coli.*** Overexpression of Aar-oxa23 reduces Oxa23-sfGFP expression by visual quantification on a plate. Oxa23-sfGFP translation is not impacted by overexpression of the nonsense sRNA on pAMCK15. Oxa23-sfGFP expression is slightly reduced by overexpression of WT scaffold sRNA Aar. Oxa23-sfGFP expression is reduced by overexpression of Aar-oxa23. Imaged on the ImageQuant LAS4000 (GE Healthcare).

**Quantification of Aar-oxa23-*oxa23* interaction *in vivo* in *E. coli* TOP10 and *A. baumannii* AB5075**

The strains pAMCK18-Oxa23 transformed with either the Aar-oxa23 overexpression plasmid (pAMCK14-Aar-oxa23), Aar overexpression (pAMCK14-Aar) or the control sRNA plasmid (pAMCK15) were then used for quantification of the change in fluorescence after 30 h in both *E. coli* and *A. baumannii* AB5075. In *E. coli*, the overexpression of the programmed sRNA Aar-oxa23 significantly reduced Oxa-23-sfGFP

fluorescence (~5.8-fold, $p < 0.0001$) when compared with the control pAMCK15 **(Figure 13 A).** Overexpression of Aar also significantly reduced Oxa-23-sfGFP fluorescence (~1.5-fold, $p < 0.0001$). There was also a significant difference in fluorescence between the overexpression of Aar-oxa23 compared to Aar ($p < 0.001$). In *A. baumannii* AB5075, Aar-oxa23 expression caused a significant reduction in fluorescence compared to the control (~1.4-fold, $p < 0.001$), while there was not a significant reduction in fluorescence from Aar compared to pAMCK15 ($p > 0.05$) **(Figure 13 B)**. A significant reduction in fluorescence was noted between Aar and Aar-oxa-23 expression in *A. baumannii* AB5075 ($p > 0.01$).

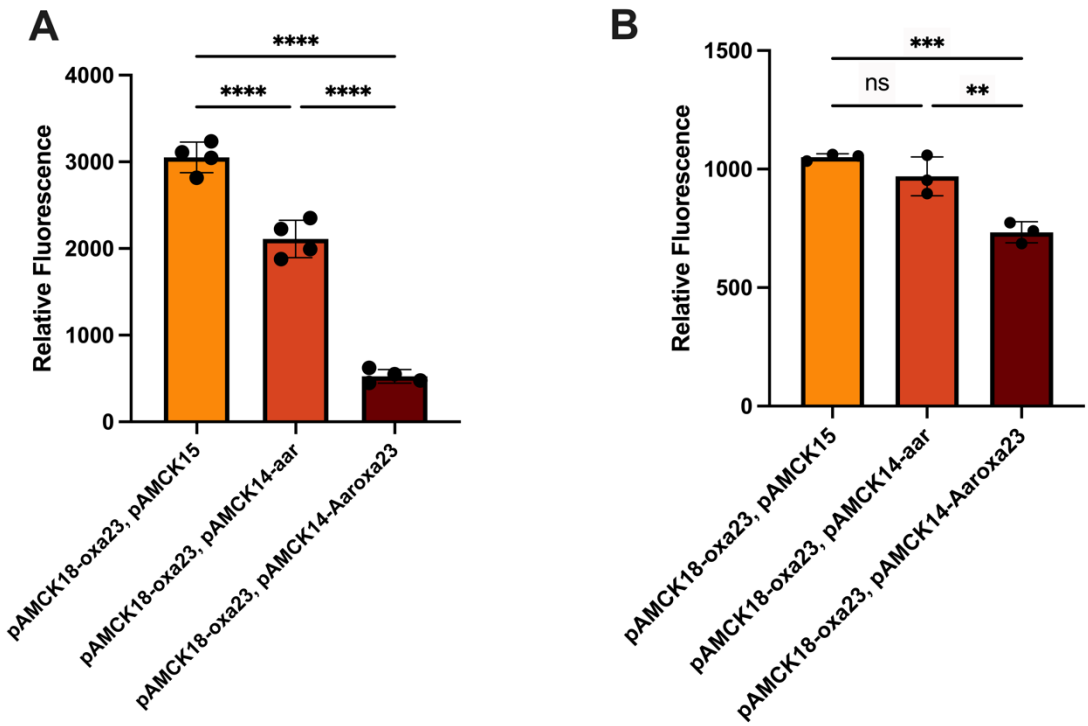


**Figure 13: Programmed sRNA Aar-oxa23 inhibits Oxa23-sfGFP expression *in vivo* in (A) *E. coli*, and (B) *A. baumannii* AB5075 measured by Oxa23-sfGFP translational reporters**. Error bars represent the standard deviation of three (B) or four (A) independent biological replicates (n=3)(n=4). Statistical analysis was performed using one-way ANOVA with Tukey's post hoc test. Significance was defined where * denotes $P<0.05$, ** denotes $P<0.01$, *** denotes $P<0.001$ and **** denotes $P<0.0001$.

**Native Aar base pairs with *Oxa-23***

Due to pAMCK14-Aar repressing Oxa-23-sfGFP in *E. coli* **(Figure 13 A),** the base pairing interaction between this pair was predicted using IntaRNA. Native Aar appears to show weak base pairing with Oxa-23 of six nucleotides **(Figure 14).** The hybridisation energy is not strong (-9.58 kcal/mol) as a more negative value suggests stronger binding.

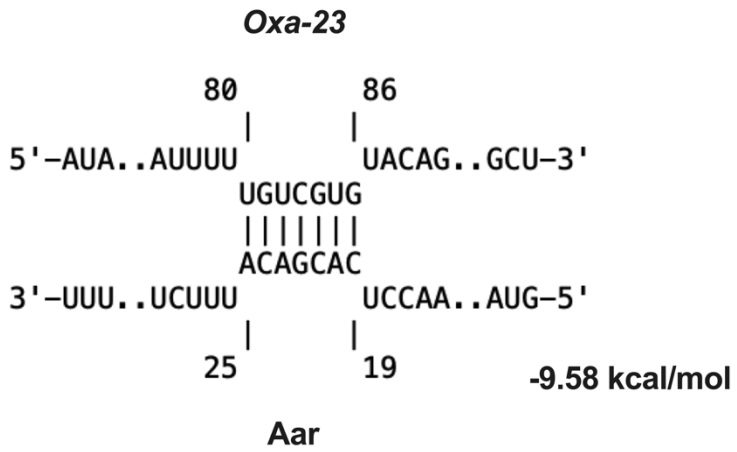


**Figure 14: Aar base pairing interaction with *oxa-23*, predicted by IntaRNA (Busch *et al.*, 2008).** The interaction has a hybridisation energy of -9.58 kcal/mol, which is relatively weak.

**Programmed sRNA Aar-oxa23 downregulates Oxa-23 protein levels in *E. coli***

To determine whether Aar-oxa23 represses Oxa-23 protein levels *in vivo* in *E. coli,* Oxa-23-sfGFP levels were compared in *E. coli* containing pAMCK18-Oxa-23 with either pAMCK15, pAMCK14-Aar or pAMCK14-Aar-oxa23 **(Figure 15 A)**. The strains were grown overnight to late stationary phase prior to preparation of whole cell lysates. Quantification of the Oxa23-sfGFP bands showed that Oxa23-sfGFP was significantly reduced in the strain overexpressing Aar compared to control pAMCK15 (~3.7-fold, $p < 0.01$) **(Figure 15 B).** Overexpression of programmable sRNA Aar-oxa23 caused an even more significant, 9.4-fold reduction in Oxa23-sfGFP when compared to the control band ($p < 0.001$)**(Figure 15 B).**

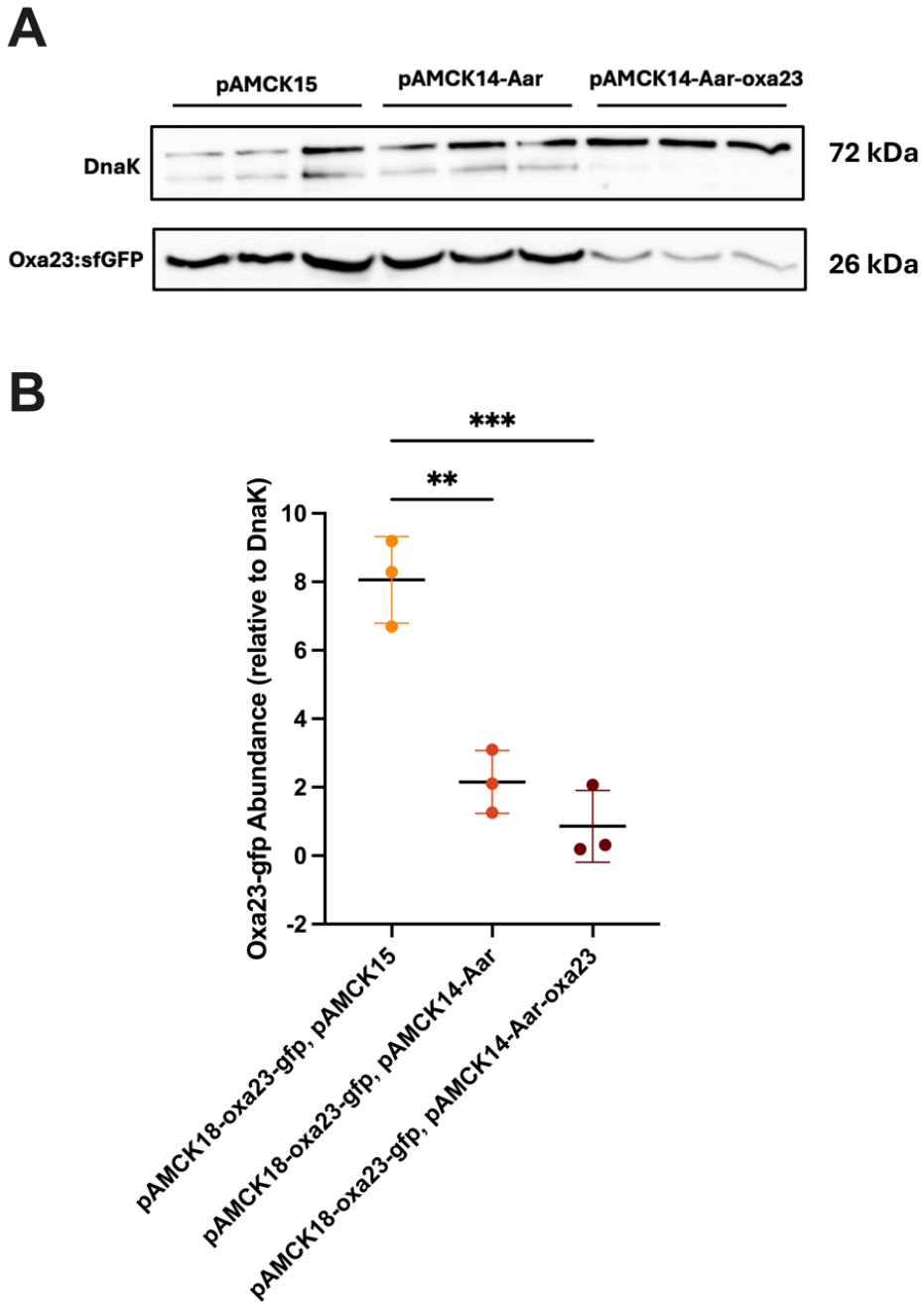


**Figure 15: Western blotting of oxa-23-sfGFP in *E.coli*.** (A) *E.coli* strains containing pAMCK18-Oxa23-sfGFp with the following plasmids were tested : pAMCK15, pAMCK14-Aar and pAMCK14-Aar-oxa23. Whole cell lysates at $OD_{600}$ = 0.05 were used for western blotting. DnaK was used as a loading control. Expression of Oxa23-sfGFP and DnaK was detected using anti-GFP and anti-DnaK antibodies. 3 biological replicates of each strain was performed (n=3). **(B) Quantification of Oxa23-sfGFP expression** relative to loading control DnaK bands from (A). Statistical tests were performed using One-way ANOVA followed by Tukey's test. Error bars represent the standard deviation from independent biological replicates. Differences were considered statistically significant where * denotes P<0.05, ** denotes P<0.01 and *** denotes *P*<0.001.

**Antibiotic susceptibility testing of programmed sRNA Aar-oxa23**

As the repression of Oxa-23 by programmed sRNA Aar-oxa23 has been validated on an RNA and protein level, it was necessary to test the effect at a phenotypic level. As Oxa-23 encodes a carbapenemase, the effect of Aar-oxa23 on carbapenem resistance was investigated. To determine if the programmable sRNA Aar-oxa23 alters the antibiotic susceptibility of *A.bauamannii* AB5075, an antibiotic disc diffusion assay was performed. *A. baumannii* AB5075 wild-type cells were transformed with the plasmid harbouring the programmed sRNA Aar-oxa23 as well as pAMCK14-Aar and the pAMCK15 control plasmid. This resulted in the creation of the strains *A. baumannii* AB5075 pAMCK15, AB5075 pAMCK14-Aar and AB5075 pAMCK14-Aar-oxa23. As Oxa-23 encodes a carbapenemase which is a beta-lactamase, beta lactam antibiotics were chosen for this assay. The beta lactam antibiotics tested were imipenem (10 µg), meropenem (10 µg), ceftazidime (30 µg) and oxacillin (1 µg) **(Figure 16**). *A. baumannii* AB5075 overexpressing the programmed sRNA Aar-oxa23 had larger zones of inhibition for carbapenems meropenem and imipenem compared to wild-type, pAMCK15 and pAMCK14-Aar strains **(Figure 16).** Aar-oxa23 significantly increased the size of zones of inhibition compared to all other strains for the carbapenems meropenem ($p < 0.01$) and imipenem ($p < 0.0001$) **(Figure 17 A,B).**

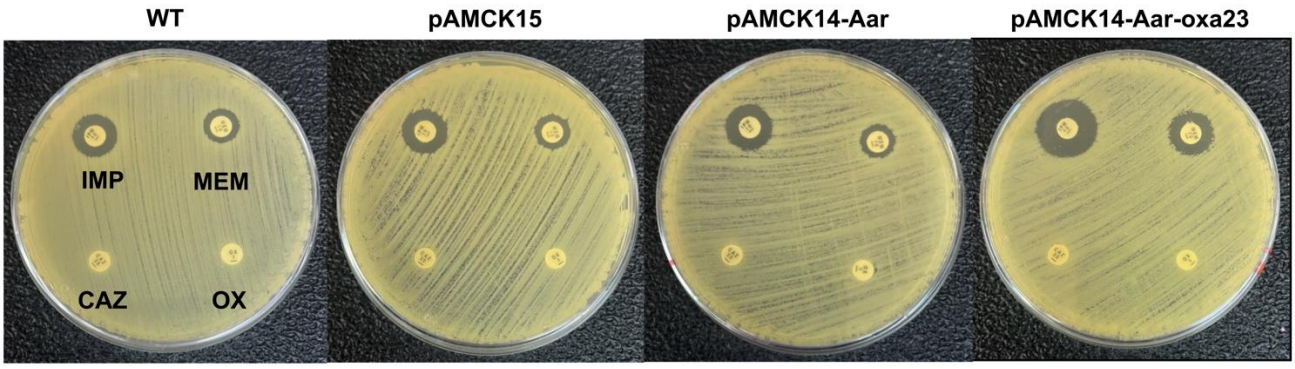


**Figure 16: Programmed sRNA Aar-oxa23 increases *A. baumannii* AB5075 wild-type susceptibility to carbapenems in antibiotic disc diffusion assay.** Strains AB5075 WT, pAMCK15, overexpression of Aar pAMCK14-Aar and overexpression of programmed sRNA pAMCK14-Aar-oxa23 were tested. Antibiotics used were imipenem (IMP)(10 µg), meropenem (MEM)(10 µg), ceftazidime (CAZ)(30 µg) and oxacillin (OX)(1 µg).

CLSI guidelines state the resistance breakpoints for meropenem is ≤ 14 mm and for imipenem is ≤ 18 mm. The intermediate breakpoints are 15-17 mm for meropenem and 19-21 for imipenem (CLSI M100 ED35:2025). The zones of inhibition from the antibiotic

disc diffusion are listed in **Table 8.** For AB5075 WT, pAMCK15 and pAMCK14-Aar the zone of inhibition for meropenem is 9-10 mm, deeming these strains resistant to meropenem. The overexpression of the programmed sRNA Aar-oxa23 increases the zone of inhibition to 13-16 mm bringing them into a resistant/intermediate range. The zone of inhibition of imipenem for the control strains was 13-14 mm, making these resistant to imipenem. The expression of Aar-oxa23 had zone of inhibition range from 18-20 mm, placing it also in resistant/ intermediate range. All strains were resistant to ceftazidime and oxacillin. These results confirm that the programmed sRNA represses the translation of Oxa-23, preventing Oxa-23 carbapenemase from being expressed, reducing *A. baumannii* AB5075 resistance to meropenem and imipenem.

**Table 8: Zones of inhibition (mm)**

| Antimicrobial Agent | WT | | | pAMCK15 | | | pAMCK14-Aar | | | pAMCK14-Aar-oxa23 | | |
|---|---|---|---|---|---|---|---|---|---|---|---|---|
| Ceftazidime | R | R | R | R | R | R | R | R | R | R | R | R |
| Oxacillin | R | R | R | R | R | R | R | R | R | R | R | R |
| Meropenem | 10 | 10 | 10 | 10 | 10 | 10 | 9 | 10 | 10 | 13 | 16 | 13 |
| Imipenem | 14 | 14 | 14 | 13 | 14 | 13 | 14 | 14 | 14 | 18 | 20 | 18 |

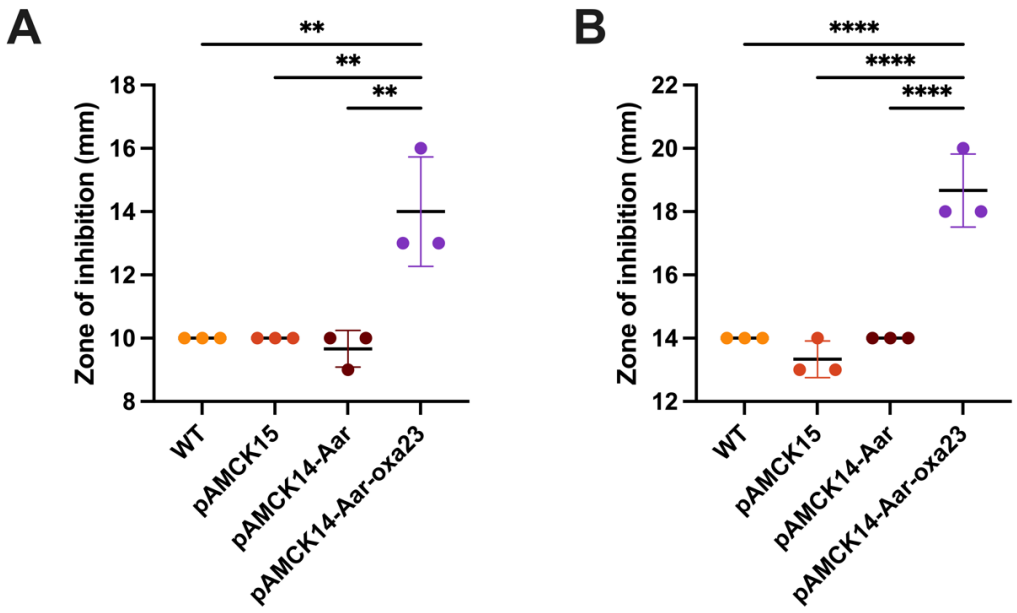


**Figure 17: Programmed sRNA Aar-oxa23 increases *A. baumannii* AB5075 susceptibility to (A) meropenem and (B) imipenem.** Error bars represent the standard deviation of three independent biological replicates (n=3). Statistical analysis was performed using one-way ANOVA with Tukey's post hoc test. Significance was defined where * denotes $P<0.05$, ** denotes $P<0.01$, *** denotes $P<0.001$ and **** denotes $P<0.0001$.

# Discussion

## Chapter 1

The post-transcriptional landscape of the ESKAPE pathogen *A. baumannii* is currently not well defined (Kröger *et al.*, 2016). However recent advancements in RNA biology including the development of new techniques such as Hi-GRIL-seq have allowed for the discovery of novel sRNAs and their target mRNAs in *A. baumannii* AB5075 (Hamrock *et al.*, 2024). This previous study uncovered the sRNA-mRNA interaction of Arp with *pilA* mRNA (Hamrock *et al.*, 2024). The gene *pilA* encodes the major pilin subunit PilA in T4P which is involved in the interlinked phenotypes of twitching motility and DNA uptake (Mattick *et al.*, 1996, Wilharm *et al.*, 2013). This work aimed to functionally characterise the sRNA Arp in *A. baumannii* AB5075, to gain insight into the sRNA mediated genetic control of *A. baumannii*.

Initially, bioinformatic predictions of the Arp-*pilA* interaction (**Figure 2**) were verified *in vivo* in this study in both *E. coli* and *A. baumannii* using the newly created pAMCK plasmid system (**Figure 4**). A potential Arp interacting region had previously been identified to be four cytosine nucleotides located at the top of the second loop of the predicted structure of Arp (**Figure 2)**. Mutation of this interacting region was shown to alleviate the repression of PilA by Arp *in vivo* in both *A. baumannii* and *E.coli* **(Figure 4).** Compensatory mutations in PilA were predicted to re-initiate this sRNA-mRNA interaction, however the disruption of the *pilA* SD sequence prevented translation of *pilA*-sfGFP and therefore no fluorescence was detected. Confirming the interaction of Arp-*pilA* in *A. baumannii* furthers confidence in the importance of this interaction, however the full mechanism is yet to be understood. To address this, direct basepairing between Arp and *pilA* mRNA must be confirmed. It is also necessary to investigate the potential role of the RNA chaperone Hfq in this interaction, as it has shown to be important for many *A. baumannii* cellular processes (Sharma *et al.*, 2018).

Arp was then shown to have a role in the regulation of T4P-mediated phenotypes. Arp was shown to be a repressor of twitching motility with wild-type levels of Arp downregulating this phenotype and the deletion of Arp showing an increase in twitching

motility **(Figure 5).** Despite the interaction between Arp-*pilA* being confirmed, it must also be considered that *trans*-acting sRNAs often have multiple target mRNAs which are involved in one pathway. Therefore the deletion of Arp may affect other mRNAs other than *pilA* which contribute to this phenotype**.** Further, understanding the conditions and environments which trigger the induction or repression of this phenotype are also key to uncovering the biological role of this sRNA. Uncovering what cues and conditions cause the bacteria to initiate twitching motility would provide valuable insight into RNA biology. In *A. baumannii*, surface-associated motility is more well characterised, with research showing that the phenotype is regulated by blue light and quorum sensing (Tuttobene *et al.*, 2021). It would be worthwhile to investigate if similar cues are also involved in twitching motility.

Twitching motility and DNA uptake are linked T4P activities and *A. baumannii* is a naturally competent bacterium. The role of Arp as a regulator of natural competence in *A. baumannii* was also investigated. The overexpression of Arp *in vivo* in *A. baumannii* completely eliminated the phenotype suggesting Arp is a repressor of DNA uptake **(Figure 6).** However, the deletion of Arp shows similar levels of DNA uptake compared to wild-type **(Figure 6)**. No noticeable reduction of DNA uptake in the Arp deletion mutant could be due to the fact that pilus production is growth phase dependent and transformability was tested at 3 h where *pilA* expression is at its peak, preventing the phenotype from being noticeable (Vesel & Blokesch, 2021). Hi-GRIL-seq data that revealed the Arp-*pilA* interaction was acquired at early stationary phase, it is possible that Arp is not expressed in the exponential phase when competence occurs (Vesel & Blokesch, 2021, Hamrock, 2025). Determining the quantity of PilA via western blot in an Arp deletion strain at different growth stage could show if Arp is responsible for the repression of PilA in stationary phase which has been previously noted (Vesel & Blokesch, 2021). Arp may not be expressed in exponential growth phase, allowing for *pilA* to be translated and T4P phenotypes to occur. Stationary phase may cause for expression of Arp, downregulating translation of *pilA*, preventing transformation and motility. It has been revealed that T4P biogenesis is subject to information from two component system PilSR and chemosensory system Pil-Chp (Vesel & Blokesch, 2021). Arp may work alongside these systems to quickly regulate pilus production in stressful conditions. Further studies would investigate the conditions under which Arp is produced and regulates these phenotypes. It seems Arp is not crucial in exponential phase when

twitching motility and horizontal gene transfer allow the bacterium to explore the environment and uptake environmental DNA such as antibiotic resistance determinants, or respond to the limiting conditions such as starvation or desiccation. Conversely, it is possible that Arp represses *pilA* during exponential and early stationary phase, but that this is derepressed at some stage during the overnight incubation leading to increased transformability. The transformation media may also play role, perhaps preventing Arp expression, leading to the differences between transformability and motility noted.

In conclusion, there is strong evidence to suggest Arp is a sRNA involved in the regulation of twitching motility and DNA uptake. Arp has been shown to bind to *pilA* mRNA, repressing its translation, which may be responsible for these phenotypes. Further investigation is needed to fully elucidate this mechanism, as well as determining if Hfq is involved in this regulation. There is also potential for Arp as a target for therapeutics, such as antisense oligonucleotides which could suppress horizontal gene transfer and the uptake of antibiotic resistance determinants.

**Chapter 2**

Carbapenem resistant *A. baumannii* (CRAb) is a pathogen of global concern and a critical priority for discovery and research into new antibiotics (Sati *et al.*, 2025). With the lack of new antibiotic discovered in recent years, new approaches and therapeutics need to be considered to combat antibiotic resistance. Programmable RNA-based antibiotics offer a promising avenue for new synthetic therapeutics, yet need more investigation (Vogel, 2020).

Many mechanisms of bacterial antibiotic resistance have emerged, a common type of resistance found in *A. baumannii* is the production of beta-lactamases, enzymes which render beta-lactam antibiotics ineffective. Oxa-23 is a carbapenemase which is a leading cause of carbapenem resistance in *A. baumannii* (Mack *et al.*, 2025). In order to combat this resistance mechanism, there is a need for new beta lactamase inhibitors (Bush & Bradford, 2020). One such therapeutic could be programmed RNA-antibiotics in the form of antisense oligonucleotides (ASOs), which could bind to the mRNA transcripts of these enzymes, supressing their translation. By targeting and downregulating beta-lactamases,

highly antibiotic resistant strains could become less virulent and more susceptible to already available antibiotics. This could extend the shelf life of the current antibiotics without having to go through the process of drug discovery for new antibiotics.

Some studies have investigated the effectiveness of synthetic sRNAs at altering mRNA translation in bacteria, for example, a study by Na *et al.,* (2013) used synthetic sRNA to metabolically engineer *E. coli* (Na *et al.*, 2013). The therapeutic potential of synthetic sRNAs to suppress virulence factors has also been investigated with a targeted and high-throughput gene knockdown system in diverse bacteria using synthetic sRNAs (Cho *et al.*, 2023). As sRNAs are often involved in the fine tuning of the stress response to environmental conditions, some sRNAs function in the control antibiotic resistance, such as MicF which regulates carbenicillin resistance in *E. coli* and RyhB which was also found to regulate sensitivity to colicin (Salvail *et al.*, 2013). Therefore, sRNAs have also been tested as targets for ASOs, such as MicF in *E. coli* (Tsai *et al.*, 2023).

Understanding the mechanisms of natural sRNA is crucial to the development of synthetic sRNA antibiotics. Synthetic programmable sRNAs can leverage the natural function of sRNAs to regulate gene translation of a target gene of choice. This study aimed to create a programmable sRNA which targets the carbapenemase Oxa-23 in CRAb AB5075, thereby making this multi-drug resistant strain susceptible to carbapenems. To test the potential of Oxa-23 as a target for programmed sRNA antibiotics, the pAMCK plasmid system was used and proved sufficient to test the effectiveness of the programmed sRNA at binding and downregulating Oxa-23.

To evaluate known sRNAs as potential sRNA scaffolds for programmable RNA-antibiotics, RyhB-2 and Aar were investigated in *A. baumannii* AB5075. In *E. coli*, RyhB-2 showed repression of SodB *in vivo*, however, the same was not found in *A. baumannii* (**Figure 8).** It was considered that the interaction may work in a growth phase dependent manner, therefore the interaction was investigated over 30 h however, it was confirmed that no other time point shows a change in the level of fluorescence for this interaction in *A. baumannii* (**Figure 9).** *Salmonella enterica* RyhB-2 is a paralog of RyhB found in *E. coli* which requires Hfq to bind to its targets (Massé & Gottesman, 2002). *Salmonella enterica* and *E. coli* Hfq share 94% similarity at the nucleotide and amino acid level, which could be allowing this interaction to work in the *E. coli* system but not *A.*

*baumannii* (Sittka *et al.*, 2007, Brown & Elliott, 1996). *A.baumannii* Hfq has an enlarged glycine rich C-terminal compared to *E. coli* Hfq, and was shown to participate in the *A. baumannii* RyhB-*sodB* interaction in Hfq-deficient *E. coli* cells. (Sharma *et al.*, 2018). Further investigation is necessary to understand this disparity.

The interaction between Aar and CarO was verified in both *E. coli* and *A. baumannii* **(Figure 8)**. The level of fluorescence was higher in *E. coli* compared to *A. baumannii* and the reduction in fluorescence in the *A. baumannii* model is less significant than in *E. coli* **(Figure 8).** This may be due to different levels of transcription or plasmid copy numbers, which could be investigated via northern blot or qPCR. There may also be endogenous chromosomally encoded regulators only found in *A. baumannii* and not *E. coli.*

Aar was chosen as the scaffold sRNA for programmable sRNA as it showed compatibility with the pAMCK system in *A.baumannii* AB5075 when binding to its known target CarO, unlike *Salmonella* RyhB-2 with SodB (**Figure 10**). The seed region of Aar is also in the typical linear region of the sRNA which makes the altering of the seed region more predictable as it is not interfering with other regions of the sRNA such as the termination loop **(Figure 11).** Within Aar, twelve nucleotides were chosen as the "seed" region and changed to bind to the new target Oxa-23, this programmed sRNA was termed "Aar-oxa23". The programmable sRNA successfully repressed the fluorescence of Oxa23-sfGFP, suggesting that changing the seed sequence with Aar as a scaffold is sufficient to target Oxa-23 (**Figure 12).** Further investigation should involve the reduction of the seed region nucleotide by nucleotide to determine the optimal or shortest seed region length possible and at what point the effect is hindered. It would also be beneficial to check if Aar-oxa23 still binds to CarO or if the altering of the seed region results in the loss of CarO as a target. This could provide overall important mechanistic insights into *Acinetobacter* sRNAs.

Aar-oxa23 significantly downregulated the expression of Oxa-23 *in vivo* in *E. coli* and *A. baumannii* AB5075 (**Figure 13**). When investigating the programmed sRNA Aar-oxa23, Aar was used as another control sRNA along with pAMCK15. The Overexpression of Aar in the *E. coli* plasmid system model showed a significant level of reduction of fluorescence, however this was eliminated in *A. baumannii* AB5075 **(Figure**

**13)**. This is likely due to Aar naturally showing some weak base pairing with Oxa-23 **(Figure 14).**

The translational repression of Oxa-23 shown in Figure 13 was confirmed to also downregulate protein expression in *E. coli* **(Figure 15**). The programmable sRNA Aar-oxa23 was shown to significantly reduce the expression of Oxa-23 protein, however it was not completely eliminated (**Figure 15**). Further investigation should uncover if Hfq is necessary for this interaction, if so, suboptimal positioning at Hfq may account for this result. Similar to above, a reduction in Oxa-23 was noted by the overexpression of Aar, which is also explained by figure 14. Another sRNA which does not shows any base pairing to Oxa-23 should be used as a more suitable control for future experiments.

The programmed sRNA Aar-oxa23 also proved to be phenotypically effective, increasing *A .baumannii's* susceptibility to the carbapenem antibiotics imipenem and meropenem **(Figure 16)**. Aar-oxa23 had no effect on oxacillin and ceftazidime resistance, as Oxa-23 specifically encodes a carbapenemase, only effective against carbapenems. The increase in zone of inhibitions with the use of the programmed sRNA Aar-oxa23 was significant for both meropenem and imipenem **(Figure 17).** Comparing to the CLSI disc diffusion zone of inhibition guidelines, the introduction of Aar-oxa23 brought the strains from resistant to intermediate-resistant. As noted via Western blotting, Aar-oxa23 does not completely repress the translation of Oxa-23 with some protein still being expressed, which accounts for the strain not becoming completely susceptible. Low levels of Oxa-23 are still being expressed allowing for some resistance to remain. The addition of an Oxa-23 deletion strain as a control would be beneficial to determine the level of repression caused by Aar-oxa23 compared to complete removal of the gene. This could uncover whether the translational repression of Oxa-23 by Aar-oxa23 is incomplete or there are other factors at play causing the resistance still noted. Other carbapenem-sensitive strains could have been used as controls for this experiment. These antibiotic disc diffusion assays of beta-lactam antibiotics showed the potential of this programmable sRNA to work in combination with antibiotics making them more effective to previously resistant infections. Further experimentation should include more antibiotic resistance testing, such as a minimal inhibitory concentration assay with imipenem and meropenem to gain a more quantifiable difference in resistance profiles.

This work has shown the potential of RNA-based “antibiotics” or adjuvants as a promising route for future therapeutics. In theory ASOs should have less or minimal side effects compared to traditional antibiotics. They offer a species-specific approach rather than commonly used broad spectrum antibiotics which can disrupt commensal bacteria in the host. However, the use of short sRNA sequences also comes with the potential for off-target binding within the target bacteria or other members of the microbiome. As well as this, it would be harder for bacteria to develop resistance to these therapies as ASOs target essential genes mRNA transcripts which if mutated could be detrimental to the bacteria’s virulence or life cycle. RNA-based therapies such as Aar-oxa23 used in combination with antibiotics could make resistance even more difficult, as the pathogen is being targeted from multiple sides, meaning its harder for them to overcome multiple inhibitory mechanisms at once. This type of adjunctive sRNA therapy could restore sensitivity to last-resort antibiotics such as carbapenems. This approach could be similar to CRISPR knockdown methods but just preventing translation, making resistance less likely.

However, there are also a few limitations and further considerations for this therapy, such as drug delivery systems. As mentioned before, ASOs to be used as a treatment must be attached to a cell-penetrating protein (CPP) in order to gain entry into the bacterial cell. A previous study from 2016, investigated the effectiveness of locked nucleic acids (LNAs) or bridged nucleic acids (BNAs) with external guide sequences (EGS) tethered to a CPP at reducing antibiotic resistance in *A. baumannii* A155 (Jackson *et al.*, 2016). The EGS base-paired with the amikacin resistance gene *aac(6')-Ib*, causing RNAse cleavage of the mRNA and inhibited growth in the presence of this antibiotic, showing that ASOs attached to CPPs can self-mediate entry into *A. baumannii* and have therapeutic effects. It also outlines that further investigation is still needed to determine the best kind of CPP. Further studies for the efficacy of Aar-oxa23 as a therapy would involve tethering Aar-oxa23 to a CPP to investigate its ability to enter *A. baumannii* cells in eukaryotic tissue culture.

Next steps for this research would also include the assessment of off target effects of this therapy. The distinct seed regions of the ASOs are designed to base pair with specific mRNA targets, however it is possible that they will bind to other transcripts. Therefore these therapies need to be tested in bacterial communities as well as in eukaryotic host cells. Expression levels of mRNA from the targeted species and then other species in the

microbiome should be investigated via RNA-seq to determine if the ASO are affecting other genes. It is also important to consider human cell toxicity. If the ASO can mediate entry into bacterial cells it is also likely that it can enter the host cells, potentially reaching the nucleus and causing DNA damage. The advancements of technologies such as Dual RNA-seq could provide insight into these off-target effects on the human hosts transcriptome (Westermann *et al.*, 2017).

In conclusion, this work has shown the potential of programmable sRNAs as adjunctive therapies to re-sensitise multi-drug resistant *A. baumannii* to currently available last-line antibiotics. The generation of these programmable sRNA is relatively simple and effective, yet many challenges remain in making them available as treatments. Further testing of drug delivery systems and off-target effects is essential to determining the actual possibilities of using these therapies, but could be crucial to resolving multi-drug resistant infections.

## Bibliography


Agodi, A., Auxilia, F., Barchitta, M., Brusaferro, S., D'Alessandro, D., Montagna, M.T., Orsi, G.B., Pasquarella, C., Torregrossa, V., and Suetens, C. (2010) Building a benchmark through active surveillance of intensive care unit-acquired infections: the Italian network SPIN-UTI. *Journal of Hospital Infection* **74**: 258-265.

Ahuatzin-Flores, O.E., Torres, E., and Chávez-Bravo, E. (2024) Acinetobacter baumannii, a multidrug-resistant opportunistic pathogen in new habitats: A systematic review. *Microorganisms* **12**: 644.

Ambler, R.P. (1997) The structure of β-lactamases. *Philosophical Transactions of the Royal Society of London. B, Biological Sciences* **289**: 321-331.

Bandić-Pavlović, D., Zah-Bogović, T., Žižek, M., Bielen, L., Bratić, V., Hrabač, P., Slačanac, D., Mihaljević, S., and Bedenić, B. (2020) Gram-negative bacteria as causative agents of ventilator-associated pneumonia and their respective resistance mechanisms. *J Chemother* **32**: 344-358.

Bhowmik, S., Pathak, A., Pandey, S., Devnath, K., Sett, A., Jyoti, N., Bhando, T., Akhter, J., Chugh, S., Singh, R., Sharma, T.K., and Pathania, R. (2025) Acinetobacter baumannii represses type VI secretion system through a manganese-dependent small RNA-mediated regulation. *mBio* **16**: e0302524.

Blanco, N., Harris Anthony, D., Rock, C., Johnson, J.K., Pineles, L., Bonomo Robert, A., Srinivasan, A., Pettigrew Melinda, M., and Thom Kerri, A. (2017) Risk Factors and Outcomes Associated with Multidrug-Resistant Acinetobacter baumannii upon Intensive Care Unit Admission. *Antimicrobial Agents and Chemotherapy* **62**: 10.1128/aac.01631-01617.

Brown, L., and Elliott, T. (1996) Efficient translation of the RpoS sigma factor in Salmonella typhimurium requires host factor I, an RNA-binding protein encoded by the hfq gene. *Journal of Bacteriology* **178**: 3763-3770.

Brück, M., Köbel, T., Dittmar, S., Ramírez Rojas, A., Georg, J., Berghoff, B., and Schindler, D., (2024) *A library-based approach allows systematic and rapid evaluation of seed region length and reveals design rules for synthetic bacterial small RNAs*.

Busch, A., Richter, A.S., and Backofen, R. (2008) IntaRNA: efficient prediction of bacterial sRNA targets incorporating target site accessibility and seed regions. *Bioinformatics* **24**: 2849-2856.

Bush, K., and Bradford, P.A. (2020) Epidemiology of beta-Lactamase-Producing Pathogens. *Clin Microbiol Rev* **33**.

Calderón, I.L., Morales, E.H., Collao, B., Calderón, P.F., Chahuán, C.A., Acuña, L.G., Gil, F., and Saavedra, C.P. (2014) Role of Salmonella Typhimurium small RNAs RyhB-1 and RyhB-2 in the oxidative stress response. *Research in Microbiology* **165**: 30-40.

Capodimonte, L., Meireles Fernando Teixeira, P., Bahr, G., Bonomo Robert, A., Dal Peraro, M., López, C., and Vila Alejandro, J. (2024) OXA β-lactamases from Acinetobacter spp. are membrane bound and secreted into outer membrane vesicles. *mBio* **16**: e03343-03324.

Chauvier, A., and Walter, N.G. (2024) Regulation of bacterial gene expression by non-coding RNA: It is all about time! *Cell Chemical Biology* **31**: 71-85.

Cho, J.S., Yang, D., Prabowo, C.P.S., Ghiffary, M.R., Han, T., Choi, K.R., Moon, C.W., Zhou, H., Ryu, J.Y., Kim, H.U., and Lee, S.Y. (2023) Targeted and high-throughput gene knockdown in diverse bacteria using synthetic sRNAs. *Nature Communications* **14**: 2359.

Chung, D.R., Song, J.-H., Kim, S.H., Thamlikitkul, V., Huang, S.-G., Wang, H., So, T.M.-k., Yasin, R.M.D., Hsueh, P.-R., Carlos, C.C., Hsu, L.Y., Buntaran, L., Lalitha, M.K., Kim, M.J., Choi, J.Y., Kim, S.I., Ko, K.S., Kang, C.-I., and Peck, K.R. (2011) High Prevalence of Multidrug-Resistant Nonfermenters in Hospital-acquired Pneumonia in Asia. *American Journal of Respiratory and Critical Care Medicine* **184**: 1409-1417.

Corcoran, C.P., Podkaminski, D., Papenfort, K., Urban, J.H., Hinton, J.C.D., and Vogel, J. (2012) Superfolder GFP reporters validate diverse new mRNA targets of the classic porin regulator, MicF RNA. *Molecular Microbiology* **84**: 428-445.

Craig, L., Forest, K.T., and Maier, B. (2019) Type IV pili: dynamics, biophysics and functional consequences. *Nature Reviews Microbiology* **17**: 429-440.

Da Silva, G.J., and Domingues, S., (2016) Insights on the Horizontal Gene Transfer of Carbapenemase Determinants in the Opportunistic Pathogen Acinetobacter baumannii. In: Microorganisms. pp.

Davis, K., Moran, K., McAllister, C.K., and Gray, P. (2005) Multidrug-Resistant Acinetobacter Extremity Infections in Soldiers. *Emerging Infectious Disease journal* **11**: 1218.

de Dios, R., Gadar, K., and McCarthy, R.R. (2022) A high-efficiency scar-free genome-editing toolkit for Acinetobacter baumannii. *J Antimicrob Chemother* **77**: 3390-3398.

De Oliveira, D.M., Forde, B.M., Kidd, T.J., Harris, P.N., Schembri, M.A., Beatson, S.A., Paterson, D.L., and Walker, M.J. (2020) Antimicrobial resistance in ESKAPE pathogens. *Clinical microbiology reviews* **33**: 10.1128/cmr. 00181-00119.

de Souza, J., D'Espindula, H.R.S., Ribeiro, I.F., Gonçalves, G.A., Pillonetto, M., and Faoro, H. (2025) Carbapenem Resistance in Acinetobacter baumannii: Mechanisms, Therapeutics, and Innovations. *Microorganisms* **13**.

Dersch, P., Khan, M.A., Mühlen, S., and Görke, B. (2017) Roles of Regulatory RNAs for Antibiotic Resistance in Bacteria and Their Potential Value as Novel Drug Targets. *Frontiers in Microbiology* **Volume 8 - 2017**.

Dias, N., and Stein, C.A. (2002) Antisense Oligonucleotides: Basic Concepts and Mechanisms. *Molecular Cancer Therapeutics* **1**: 347-355.

Donald, H.M., Scaife, W., Amyes, S.G., and Young, H.K. (2000) Sequence analysis of ARI-1, a novel OXA beta-lactamase, responsible for imipenem resistance in Acinetobacter baumannii 6B92. *Antimicrob Agents Chemother* **44**: 196-199.

Eijkelkamp, B.A., Hassan, K.A., Paulsen, I.T., and Brown, M.H. (2011) Investigation of the human pathogen Acinetobacter baumannii under iron limiting conditions. *BMC Genomics* **12**: 126.

Espinal, P., Martí, S., and Vila, J. (2012) Effect of biofilm formation on the survival of Acinetobacter baumannii on dry surfaces. *Journal of Hospital Infection* **80**: 56-60.

Evans, B.A., and Amyes, S.G. (2014) OXA beta-lactamases. *Clin Microbiol Rev* **27**: 241-263.

García-Garmendia, J.-L., Ortiz-Leyba, C., Garnacho-Montero, J., Jiménez-Jiménez, F.-J., Pérez-Paredes, C., Barrero-Almodóvar, A.E., and Miner, M.G. (2001) Risk Factors for Acinetobacter baumannii Nosocomial Bacteremia in Critically Ill Patients: A Cohort Study. *Clinical Infectious Diseases* **33**: 939-946.

Gebhardt, M.J., Farland, E.A., Basu, P., Macareno, K., Melamed, S., and Dove, S.L. (2023) Hfq-licensed RNA–RNA interactome in Pseudomonas aeruginosa reveals a keystone sRNA. *Proceedings of the National Academy of Sciences* **120**: e2218407120.

Godeux, A.-S., Svedholm, E., Barreto, S., Potron, A., Venner, S., Charpentier, X., and Laaberki, M.-H. (2022) Interbacterial Transfer of Carbapenem Resistance and Large

Antibiotic Resistance Islands by Natural Transformation in Pathogenic Acinetobacter. *mBio* **13**: e02631-02621.

Gorski, S.A., Vogel, J., and Doudna, J.A. (2017) RNA-based recognition and targeting: sowing the seeds of specificity. *Nat Rev Mol Cell Biol* **18**: 215-228.

Gottesman, S., McCullen, C., Guillier, M., Vanderpool, C., Majdalani, N., Benhammou, J., Thompson, K., FitzGerald, P., Sowa, N., and FitzGerald, D., (2006) Small RNA regulators and the bacterial response to stress. In: Cold Spring Harbor symposia on quantitative biology. Cold Spring Harbor Laboratory Press, pp. 1-11.

Hamrock, F., (2025) Characterising the small RNA- regulatory architecture of Acinetobacter baumannii. In., pp.

Hamrock, Fergal J., Ryan, D., Shaibah, A., Ershova, Anna S., Mogre, A., Sulimani, Maha M., Ben Taarit, S., Reichardt, S., Hokamp, K., Westermann, Alexander J., and Kröger, C. (2024) Global analysis of the RNA–RNA interactome in Acinetobacter baumannii AB5075 uncovers a small regulatory RNA repressing the virulence-related outer membrane protein CarO. *Nucleic Acids Research* **52**: 11283-11300.

Harding Christian, M., Tracy Erin, N., Carruthers Michael, D., Rather Philip, N., Actis Luis, A., and Munson Robert, S. (2013) Acinetobacter baumannii Strain M2 Produces Type IV Pili Which Play a Role in Natural Transformation and Twitching Motility but Not Surface-Associated Motility. *mBio* **4**: 10.1128/mbio.00360-00313.

Harding, C.M., Hennon, S.W., and Feldman, M.F. (2018) Uncovering the mechanisms of Acinetobacter baumannii virulence. *Nat Rev Microbiol* **16**: 91-102.

Harding, C.M., Tracy, E.N., Carruthers, M.D., Rather, P.N., Actis, L.A., and Munson, R.S. (2013) Acinetobacter baumannii Strain M2 Produces Type IV Pili Which Play a Role in Natural Transformation and Twitching Motility but Not Surface-Associated Motility. *mBio* **4**: 10.1128/mbio.00360-00313.

Hazen, J.E., Di Venanzio, G., Hultgren, S.J., and Feldman, M.F. (2023) Catheterization of mice triggers resurgent urinary tract infection seeded by a bladder reservoir of Acinetobacter baumannii. *Science Translational Medicine* **15**: eabn8134.

Henrichsen, J., and Blom, J. (1975) Correlation between twitching motility and possession of polar fimbriae in Acinetobacter calcoaceticus. *Acta Pathol Microbiol Scand B* **83**: 103-115.

Hör, J., Gorski, S.A., and Vogel, J. (2018) Bacterial RNA Biology on a Genome Scale. *Molecular Cell* **70**: 785-799.

Jackson, A., Jani, S., Davies-Sala, C., Soler-Bistué, A.J.C., Zorreguieta, A., and Tolmasky, M.E. (2016) Assessment of configurations and chemistries of bridged nucleic acids-containing oligomers as external guide sequences: a methodology for inhibition of expression of antibiotic resistance genes. *Biology Methods and Protocols* **1**: bpw001.

Jacobs, A.C., Thompson, M.G., Black, C.C., Kessler, J.L., Clark, L.P., McQueary, C.N., Gancz, H.Y., Corey, B.W., Moon, J.K., Si, Y., Owen, M.T., Hallock, J.D., Kwak, Y.I., Summers, A., Li, C.Z., Rasko, D.A., Penwell, W.F., Honnold, C.L., Wise, M.C., Waterman, P.E., Lesho, E.P., Stewart, R.L., Actis, L.A., Palys, T.J., Craft, D.W., and Zurawski, D.V. (2014) AB5075, a Highly Virulent Isolate of Acinetobacter baumannii, as a Model Strain for the Evaluation of Pathogenesis and Antimicrobial Treatments. *mBio* **5**: e01076-01014.

Jang, T.N., Lee, S.H., Huang, C.H., Lee, C.L., and Chen, W.Y. (2009) Risk factors and impact of nosocomial Acinetobacter baumannii bloodstream infections in the adult intensive care unit: a case–control study. *Journal of Hospital Infection* **73**: 143-150.

Jaruratanasirikul, S., Nitchot, W., Wongpoowarak, W., Samaeng, M., and Nawakitrangsan, M. (2019) Population pharmacokinetics and Monte Carlo simulations of sulbactam to optimize dosage regimens in patients with ventilator-associated pneumonia caused by Acinetobacter baumannii. *Eur J Pharm Sci* **136**: 104940.

Jayaraman, K., McParland, K., Miller, P., and Ts'o, P.O.P. (1981) Selective inhibition of Escherichia coli protein synthesis and growth by nonionic oligonucleotides complementary to the 3′ end of 16S rRNA*. *Proceedings of the National Academy of Sciences* **78**: 1537-1541.

Jiang, Y., Ding, Y., Wei, Y., Jian, C., Liu, J., and Zeng, Z. (2022) Carbapenem-resistant Acinetobacter baumannii: A challenge in the intensive care unit. *Frontiers in Microbiology* **Volume 13 - 2022**.

Johansen, J., Rasmussen, A.A., Overgaard, M., and Valentin-Hansen, P. (2006) Conserved small non-coding RNAs that belong to the sigmaE regulon: role in down-regulation of outer membrane proteins. *J Mol Biol* **364**: 1-8.

Johnson, E.N., Burns, T.C., Hayda, R.A., Hospenthal, D.R., and Murray, C.K. (2007) Infectious complications of open type III tibial fractures among combat casualties. *Clin Infect Dis* **45**: 409-415.

Keen, E.F., Robinson, B.J., Hospenthal, D.R., Aldous, W.K., Wolf, S.E., Chung, K.K., and Murray, C.K. (2010) Prevalence of multidrug-resistant organisms recovered at a military burn center. *Burns* **36**: 819-825.

Kröger, C., Kary, S.C., Schauer, K., and Cameron, A.D. (2016) Genetic Regulation of Virulence and Antibiotic Resistance in Acinetobacter baumannii. *Genes (Basel)* **8**.

Kröger, C., MacKenzie, K.D., Alshabib, E.Y., Kirzinger, M.W B., Suchan, D.M., Chao, T.-C., Akulova, V., Miranda-CasoLuengo, A.A., Monzon, V.A., Conway, T., Sivasankaran, S.K., Hinton, J.C D., Hokamp, K., and Cameron, Andrew D S. (2018) The primary transcriptome, small RNAs and regulation of antimicrobial resistance in Acinetobacter baumannii ATCC 17978. *Nucleic Acids Research* **46**: 9684-9698.

Kyriakidis, I., Vasileiou, E., Pana, Z.D., and Tragiannidis, A., (2021) Acinetobacter baumannii Antibiotic Resistance Mechanisms. In: Pathogens. pp.

Köbel, T.S., Melo Palhares, R., Fromm, C., Szymanski, W., Angelidou, G., Glatter, T., Georg, J., Berghoff, B.A., and Schindler, D. (2022) An Easy-to-Use Plasmid Toolset for Efficient Generation and Benchmarking of Synthetic Small RNAs in Bacteria. *ACS Synth Biol* **11**: 2989-3003.

Mack, R., Hujer Andrea, M., Mojica Maria, F., Taracila Magdalena, A., Feldgarden, M., Haft Daniel, H., Klimke, W., Prasad Arjun, B., and Bonomo Robert, A. (2025) β-Lactamase diversity in Acinetobacter baumannii. *Antimicrobial Agents and Chemotherapy* **69**: e00784-00724.

Massé, E., and Gottesman, S. (2002) A small RNA regulates the expression of genes involved in iron metabolism in Escherichia coli. *Proceedings of the National Academy of Sciences* **99**: 4620-4625.

Mathai, A.S., Oberoi, A., Madhavan, S., and Kaur, P. (2012) Acinetobacter infections in a tertiary level intensive care unit in northern India: Epidemiology, clinical profiles and outcomes. *Journal of Infection and Public Health* **5**: 145-152.

Mattick, J.S. (2002) Type IV pili and twitching motility. *Annu Rev Microbiol* **56**: 289-314.

Mattick, J.S., Whitchurch, C.B., and Alm, R.A. (1996) The molecular genetics of type-4 fimbriae in Pseudomonas aeruginosa-a review. *Gene* **179**: 147-155.

McBride Mark, J. (2010) Shining a Light on an Opportunistic Pathogen. *Journal of Bacteriology* **192**: 6325-6326.

Melamed, S., Peer, A., Faigenbaum-Romm, R., Gatt, Y.E., Reiss, N., Bar, A., Altuvia, Y., Argaman, L., and Margalit, H. (2016) Global Mapping of Small RNA-Target Interactions in Bacteria. *Mol Cell* **63**: 884-897.

Mizuno, T., Chou, M.Y., and Inouye, M. (1984) A unique mechanism regulating gene expression: translational inhibition by a complementary RNA transcript (micRNA). *Proc Natl Acad Sci U S A* **81**: 1966-1970.

Mogre, A., Connell, O., White, J., Shaibah, A., Hokamp, K., Hamrock, F.J., Schauer, K., and Kröger, C. (2025) Development of two compatible plasmids to assess sRNA-mediated post-transcriptional regulation in Acinetobacter baumannii. *bioRxiv*: 2025.2007.2011.664372.

Mohd Sazlly, S., Zainal Abidin, A., Liew, S.M., Roberts, J.A., and Sime, F.B. (2019) The global prevalence of multidrug-resistance among Acinetobacter baumannii causing hospital-acquired and ventilator-associated pneumonia and its associated mortality: A systematic review and meta-analysis. *Journal of Infection* **79**: 593-600.

Na, D., Yoo, S.M., Chung, H., Park, H., Park, J.H., and Lee, S.Y. (2013) Metabolic engineering of Escherichia coli using synthetic small regulatory RNAs. *Nature Biotechnology* **31**: 170-174.

Orr, R.M. (2001) Technology evaluation: fomivirsen, Isis Pharmaceuticals Inc/CIBA vision. *Current opinion in molecular therapeutics* **3**: 288-294.

Papenfort, K., Bouvier, M., Mika, F., Sharma, C.M., and Vogel, J. (2010) Evidence for an autonomous 5′ target recognition domain in an Hfq-associated small RNA. *Proceedings of the National Academy of Sciences* **107**: 20435-20440.

Papenfort, K., and Melamed, S. (2023) Small RNAs, Large Networks: Posttranscriptional Regulons in Gram-Negative Bacteria. *Annu Rev Microbiol* **77**: 23-43.

Papenfort, K., Pfeiffer, V., Lucchini, S., Sonawane, A., Hinton, J.C., and Vogel, J. (2008) Systematic deletion of Salmonella small RNA genes identifies CyaR, a conserved CRP-dependent riboregulator of OmpX synthesis. *Mol Microbiol* **68**: 890-906.

Papenfort, K., Pfeiffer, V., Mika, F., Lucchini, S., Hinton, J.C.D., and Vogel, J. (2006) σE-dependent small RNAs of Salmonella respond to membrane stress by accelerating global omp mRNA decay. *Molecular Microbiology* **62**: 1674-1688.

Paton, R., Miles, R.S., Hood, J., Amyes, S.G.B., Miles, R.S., and Amyes, S.G.B. (1993) ARI 1: β-lactamase-mediated imipenem resistance in Acinetobacter baumannii. *International Journal of Antimicrobial Agents* **2**: 81-87.

Peleg, A.Y., Seifert, H., and Paterson, D.L. (2008) Acinetobacter baumannii: emergence of a successful pathogen. *Clin Microbiol Rev* **21**: 538-582.

Pifer, R., and Greenberg, D.E. (2020) Antisense antibacterial compounds. *Translational Research* **223**: 89-106.

Poirel, L., and Nordmann, P. (2006) Carbapenem resistance in Acinetobacter baumannii: mechanisms and epidemiology. *Clinical Microbiology and Infection* **12**: 826-836.

Pour, N.K., Dusane, D.H., Dhakephalkar, P.K., Zamin, F.R., Zinjarde, S.S., and Chopade, B.A. (2011) Biofilm formation by Acinetobacter baumannii strains isolated from urinary tract infection and urinary catheters. *FEMS Immunology & Medical Microbiology* **62**: 328-338.

Roca, I., Espinal, P., Vila-Farres, X., and Vila, J. (2012) The Acinetobacter baumannii Oxymoron: Commensal Hospital Dweller Turned Pan-Drug-Resistant Menace. *Front Microbiol* **3**: 148.

Rodríguez-Baño, J., Cisneros, J.M., Fernández-Cuenca, F., Ribera, A., Vila, J., Pascual, A., Martínez-Martínez, L., Bou, G., Pachón, J., and Hospitalaria, G.d.E.d.I. (2004) Clinical features and epidemiology of Acinetobacter baumannii colonization and infection in Spanish hospitals. *Infection Control & Hospital Epidemiology* **25**: 819-824.

Salinas, J.H., Gordesli-Duatepe, F.P., Diaz-Sanchez, A., and Abu-Lail, N.I., (2025) Phenotypic Characterization of pilA, pilB, and pilD Mutants of Acinetobacter baumannii 5075: Impacts on Growth, Biofilm Formation, and Tazobactam Response. In: Antibiotics. pp.

Salvail, H., Caron, M.P., Bélanger, J., and Massé, E. (2013) Antagonistic functions between the RNA chaperone Hfq and an sRNA regulate sensitivity to the antibiotic colicin. *The EMBO Journal* **32**: 2764-2778-2778.

Sarshar, M., Scribano, D., Palamara, A.T., Ambrosi, C., and Masotti, A. (2022) The Acinetobacter baumannii model can explain the role of small non-coding RNAs as potential mediators of host-pathogen interactions. *Frontiers in Molecular Biosciences* **Volume 9 - 2022**.

Sati, H., Carrara, E., Savoldi, A., Hansen, P., Garlasco, J., Campagnaro, E., Boccia, S., Castillo-Polo, J.A., Magrini, E., Garcia-Vello, P., Wool, E., Gigante, V., Duffy, E., Cassini, A., Huttner, B., Pardo, P.R., Naghavi, M., Mirzayev, F., Zignol, M., Cameron, A., Tacconelli, E., and Group, W.H.O.B.P.P.L.A. (2025) The WHO Bacterial Priority Pathogens List 2024: a prioritisation study to guide research,

development, and public health strategies against antimicrobial resistance. *Lancet Infect Dis* **25**: 1033-1043.

Schilling, D., Findeiss, S., Richter, A.S., Taylor, J.A., and Gerischer, U. (2010) The small RNA Aar in Acinetobacter baylyi: a putative regulator of amino acid metabolism. *Arch Microbiol* **192**: 691-702.

Scott, P., Deye, G., Srinivasan, A., Murray, C., Moran, K., Hulten, E., Fishbain, J., Craft, D., Riddell, S., Lindler, L., Mancuso, J., Milstrey, E., Bautista, C.T., Patel, J., Ewell, A., Hamilton, T., Gaddy, C., Tenney, M., Christopher, G., Petersen, K., Endy, T., and Petruccelli, B. (2007) An Outbreak of Multidrug-Resistant Acinetobacter baumannii-calcoaceticus Complex Infection in the US Military Health Care System Associated with Military Operations in Iraq. *Clinical Infectious Diseases* **44**: 1577-1584.

Sharma, A., Dubey, V., Sharma, R., Devnath, K., Gupta, V.K., Akhter, J., Bhando, T., Verma, A., Ambatipudi, K., Sarkar, M., and Pathania, R. (2018) The unusual glycine-rich C terminus of the Acinetobacter baumannii RNA chaperone Hfq plays an important role in bacterial physiology. *Journal of Biological Chemistry* **293**: 13377-13388.

Sharma, R., Arya, S., Patil, S.D., Sharma, A., Jain, P.K., Navani, N.K., and Pathania, R. (2014) Identification of Novel Regulatory Small RNAs in Acinetobacter baumannii. *PLOS ONE* **9**: e93833.

Sittka, A., Pfeiffer, V., Tedin, K., and Vogel, J. (2007) The RNA chaperone Hfq is essential for the virulence of Salmonella typhimurium. *Mol Microbiol* **63**: 193-217.

Smith, Clyde A., Antunes, Nuno T., Stewart, Nichole K., Toth, M., Kumarasiri, M., Chang, M., Mobashery, S., and Vakulenko, Sergei B. (2013) Structural Basis for Carbapenemase Activity of the OXA-23 β-Lactamase from Acinetobacter baumannii. *Chemistry & Biology* **20**: 1107-1115.

Storz, G., Vogel, J., and Wassarman, Karen M. (2011) Regulation by Small RNAs in Bacteria: Expanding Frontiers. *Molecular Cell* **43**: 880-891.

Sully, E.K., and Geller, B.L. (2016) Antisense antimicrobial therapeutics. *Current Opinion in Microbiology* **33**: 47-55.

Tekin, R., Dal, T., Bozkurt, F., Deveci, Ö., Palancı, Y., Arslan, E., Selçuk, C.T., and Hoşoğlu, S. (2014) Risk Factors for Nosocomial Burn Wound Infection Caused by Multidrug Resistant Acinetobacter baumannii. *Journal of Burn Care & Research* **35**: e73-e80.

Touchon, M., Cury, J., Yoon, E.J., Krizova, L., Cerqueira, G.C., Murphy, C., Feldgarden, M., Wortman, J., Clermont, D., Lambert, T., Grillot-Courvalin, C., Nemec, A., Courvalin, P., and Rocha, E.P. (2014) The genomic diversification of the whole Acinetobacter genus: origins, mechanisms, and consequences. *Genome Biol Evol* **6**: 2866-2882.

Towner, K.J. (2009) Acinetobacter: an old friend, but a new enemy. *Journal of Hospital Infection* **73**: 355-363.

Troxell, B., Fink, R.C., Porwollik, S., McClelland, M., and Hassan, H.M. (2011) The Fur regulon in anaerobically grown Salmonella enterica sv. Typhimurium: identification of new Fur targets. *BMC Microbiology* **11**: 236.

Tsai, M.J., Zambrano, R.A.I., Susas, J.L., Silva, L., and Takahashi, M.K. (2023) Identifying Antisense Oligonucleotides to Disrupt Small RNA Regulated Antibiotic Resistance via a Cell-Free Transcription–Translation Platform. *ACS Synthetic Biology* **12**: 2245-2251.

Tuttobene, M.R., Müller, G.L., Blasco, L., Arana, N., Hourcade, M., Diacovich, L., Cribb, P., Tomás, M., Nieto-Peñalver, C.G., and Mussi, M.A. (2021) Blue light directly modulates the quorum network in the human pathogen Acinetobacter baumannii. *Scientific Reports* **11**: 13375.

Urban, J.H., and Vogel, J. (2007) Translational control and target recognition by Escherichia coli small RNAs in vivo. *Nucleic Acids Research* **35**: 1018-1037.

Urban, J.H., and Vogel, J. (2008) Two seemingly homologous noncoding RNAs act hierarchically to activate glmS mRNA translation. *PLoS Biol* **6**: e64.

Valentin-Hansen, P., Eriksen, M., and Udesen, C. (2004) MicroReview: The bacterial Sm-like protein Hfq: a key player in RNA transactions. *Molecular Microbiology* **51**: 1525-1533.

Vesel, N., and Blokesch, M. (2021) Pilus Production in Acinetobacter baumannii Is Growth Phase Dependent and Essential for Natural Transformation. *Journal of Bacteriology* **203**: 10.1128/jb.00034-00021.

Vogel, J. (2020) An RNA biology perspective on species-specific programmable RNA antibiotics. *Molecular Microbiology* **113**: 550-559.

Waters, L.S., and Storz, G. (2009) Regulatory RNAs in bacteria. *Cell* **136**: 615-628.

Westermann, A.J., Barquist, L., and Vogel, J. (2017) Resolving host–pathogen interactions by dual RNA-seq. *PLOS Pathogens* **13**: e1006033.

Wilharm, G., Piesker, J., Laue, M., and Skiebe, E. (2013) DNA Uptake by the Nosocomial Pathogen Acinetobacter baumannii Occurs during Movement along Wet Surfaces. *Journal of Bacteriology* **195**: 4146-4153.

Xue, X.Y., Mao, X.G., Zhou, Y., Chen, Z., Hu, Y., Hou, Z., Li, M.K., Meng, J.R., and Luo, X.X. (2018) Advances in the delivery of antisense oligonucleotides for combating bacterial infectious diseases. *Nanomedicine* **14**: 745-758.

Zhang, Y., Werling, U., and Edelmann, W. (2012) SLiCE: a novel bacterial cell extract-based DNA cloning method. *Nucleic Acids Research* **40**: e55-e55.